

CHAPTER-4

RESULTS AND DISCUSSION

4.1. X-RAY DIFFRACTOGRAM ANALYSIS

The normal (unheated) medicinal plant leaves of A: Nephafu (*Clerodendrum colebrookianum*), B: Mahaneem (*Azadirachta indica*), C: Tulsi (*Osimum sanctum*) and D: Nayantora (*Vinca rosea*) are green in colour. On heating, the samples pass through a sequence of colour changes from dark green to pale green and to reddish brown at 455K and then almost black at about 480K. Beyond 500K the leaves transform in to ashes. Again the normal (unheated) medicinal plant fruits of E: Bandordima (*Chisocheton paniculatus*), and F: Sarumoin (*Cudrania javanensis*) are both light yellow colour. On heating, the samples pass through a sequence of colour changes light yellow to pale yellow and to reddish brown at 475K and then almost black at about 505K. Beyond 540K the fruits transform in to ashes. The X-ray diffractograms of unheated, and thermally treated (annealed and quenched) leaf and fruit samples are displays in figures 4.1, 4.2, 4.3, 4.4, 4.5 and 4.6.

Each of the diffractograms consists of different integral widths and heights. In addition of these, there are a skewed shaped amorphous halo with unusual azimuthal intensity distribution too in each case. The presence of broaden peaks, instead of obtaining sharp peaks, in these diffraction patterns is attributed to the imperfection in packing and varied crystallites size in the plant leaves and fruits under study. These kinds of diffractograms are found in partially crystalline substance, which is attributed to the imperfection and varied crystallites size¹.

Only a few peaks recorded in the x-ray diffractograms (Not more than five) of the

samples indicate the semicrystalline characters of the medicinal plant leaves and fruits. The identical x-ray diffractograms of the samples infer that all four medicinal plant leaves and two fruits possess similar crystallographic characteristics.

Amongst the leaves sample the diffractograms infer that crystallinities is more in the sample B and sample C and less in the sample A.

Again the diffractogram of fruit samples E and F showed that the crystallinity is more in sample E than the sample F.

From the diffractograms result it is establish that the crystallinity is more in fruits than in leaves.

The results of annealing and quenching effects on the crystallinity of the medicinal plant leaves and fruits are summarized in the table 4.1 and table 4.2 respectively.

The XRD data reveal that it is almost immaterial whether the B and C samples are annealed or quenched at 450K. From intensity data (PI and RI) , it is found that crystallinity unaffected for heated (annealed and quenched) sample B. Disappearance of basal reflection 3.68\AA in the heated samples except B indicates irreversible dehydration of A, C and D leaves under thermal treatments²⁻⁴

Again the XRD data of fruit samples E and F which are thermally treated (annealed and quenched) at 570K. It is also found that crystallinity unaffected for heated (annealed and quenched) fruit samples.

Table 4.1: Interplaner spacings (d_{100} Å), Peak intensity (PI) and relative intensity (RI) in counts of the medicinal plant leaves sample A-Nephafu, B-Mahaneem, C-Tulsi & D-Nayantora:

Samples	Unheated				Annealed from 450				Quenched from 450			
	2 θ in degree	d_{100} in Å	P.I	R.I %	2 θ in degree	d_{100} in Å	P.I	R.I %	2 θ in degree	d_{100} in Å	P.I	R.I %
A	44.63	6.06	12	100
	20.47	4.33	12	63.3
	26.37	3.37	19	100	46.13	1.94	4	32.27	26.8	3.33	10	100
B	14.84	5.95	31	100	14.87	5.95	12	100	15.15	5.85	11	67.7
	24.29	3.67	27	96	24.32	3.66	25	97.7	24.40	3.65	18	100
	26.61	3.35	16	57.0	26.50	3.36	13	41.3	26.70	3.36	16	90.7
	38.09	2.36	8	27.9	38.14	2.36	9	28.7	38.87	2.35	6	35.4
C	14.60	6.02	23	96.0	14.80	5.94	27	100	14.90	5.93	35	100
	24.18	3.68	24	100
	26.44	3.38	23	96.0	26.68	3.36	18	35.5	26.68	3.34	18	50.7
	28.26	3.62	14	10.0
	38.02	2.35	8	60.0	38.10	2.35	19	71.60	38.28	2.35	13	37.2
D	14.48	4.79	12	25.8
	24.22	3.66	16	35.6
	26.50	3.36	45	100	26.74	2.98	8	96.1	26.70	3.34	30	100
	38.01	2.33	30	32.1	51.15	1.78	5	100	31,06	2.20	1	4.8

Table4.2: Interplanner spacings (d_{100} Å), Peak intensity (PI) and relatives intensity (RI)

in counts of the medicinal plant fruits sample E-Bandordima & F-Sarumoin:

Samples	Unheated				Annealed from 570				Quenched from 570			
	2 θ in degree	d_{100} in Å	P.I	R.I %	2 θ in degree	d_{100} in Å	P.I	R.I %	2 θ in degree	d_{100} in Å	P.I	R.I %
E	25.20	4.47	104.1	100	25.37	4.47	108.2	100	26.70	4.42	107.1	67.7
	47.50	2.78	50.02	57	47.62	2.79	52.07	59.2	49.02	2.77	51.6	100
	57.80	3.10	31.20	54.02	58.10	3.10	35.02	55.47	59.05	3.11	34.12	55.07
	72.04	3.25	39.50	37.9	73.40	3.26	41.10	38.9	71.3	3.28	40.3	35.4
F	23.50	4.02	86.01	100	23.82	4.13	87.2	100	23.79	4.10	86.1	100
	50.02	1.78	40.10	45.54	51.10	1.82	42.10	46.30	51.30	1.76	41.7	45.20
	72.07	1.33	43.30	58.07	74.60	1.35	44.50	59.01	73.90	1.36	44	58.50

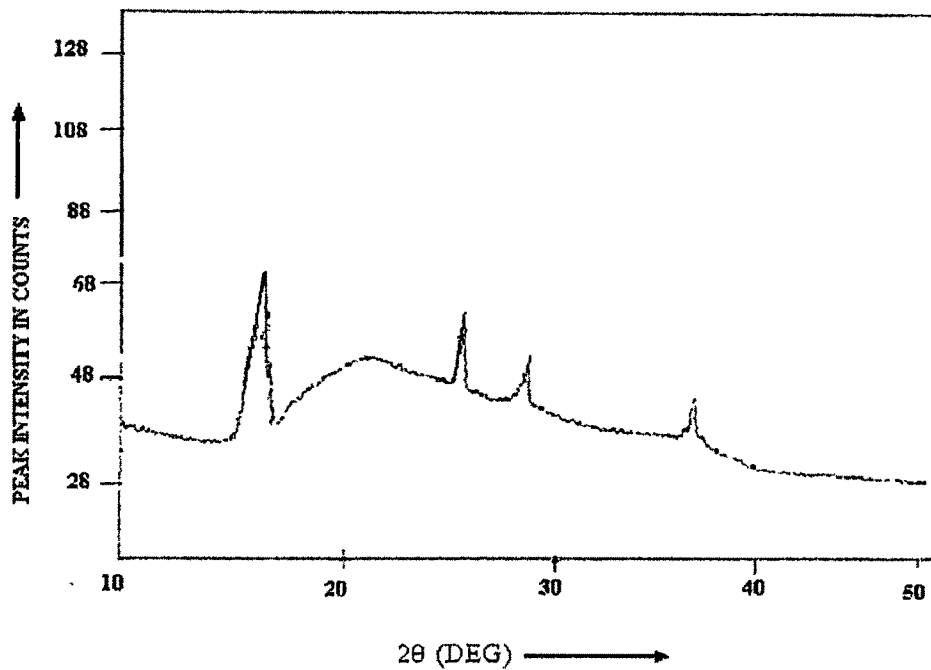


Figure 4.1(a) X-ray diffractogram of unheated sample-A

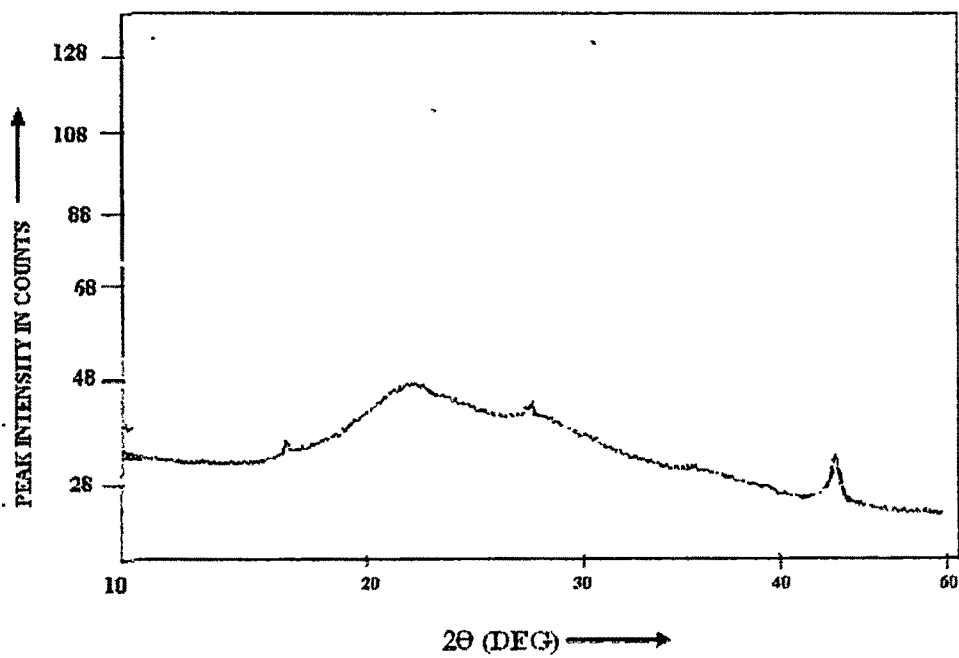


Figure 4.1(b): X-ray diffractogram of annealed sample-A

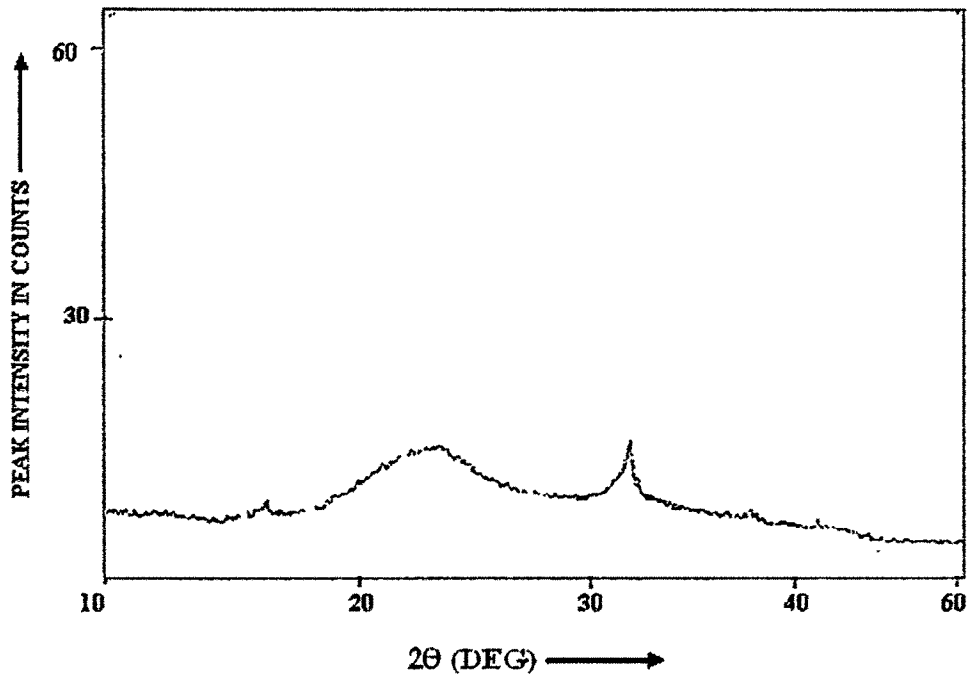


Figure 4.1(c): X-ray diffractogram of quenched sample-A

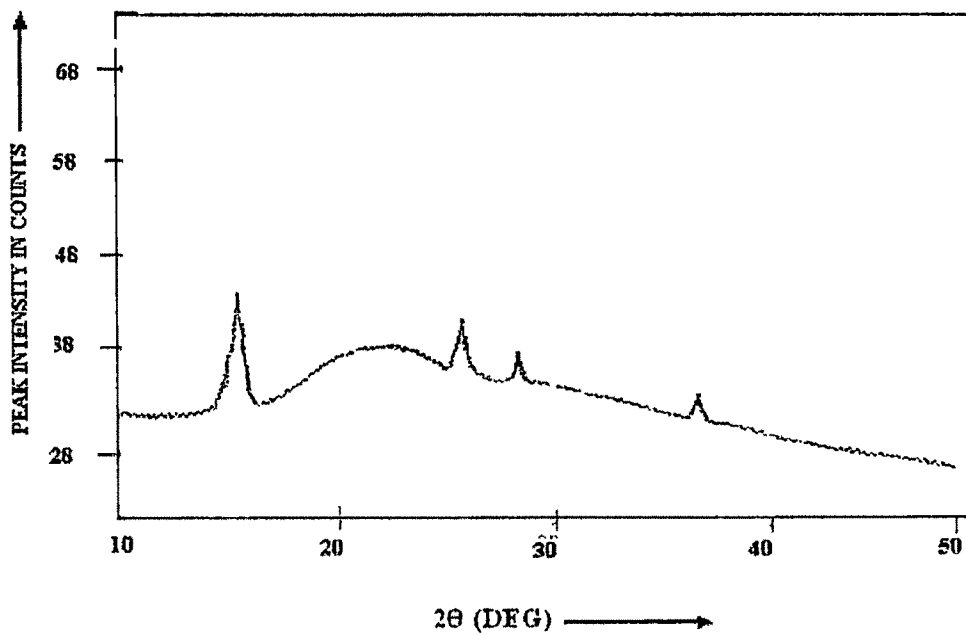


Figure 4.2(a): X-ray diffractogram of unheated sample-B

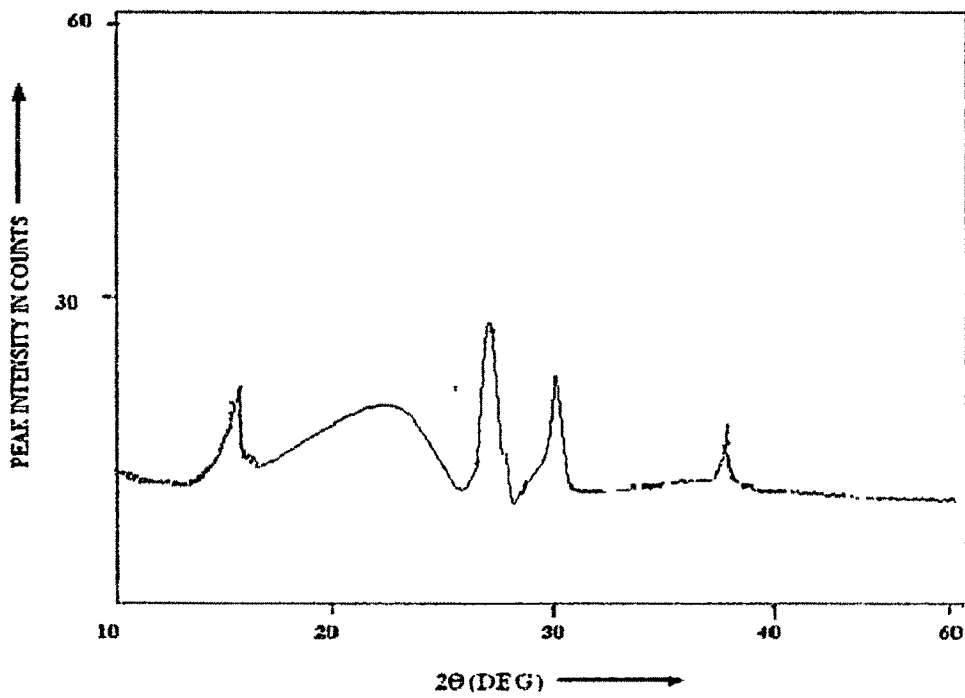


Figure 4.2(b) X-ray diffractogram of annealed sample-B

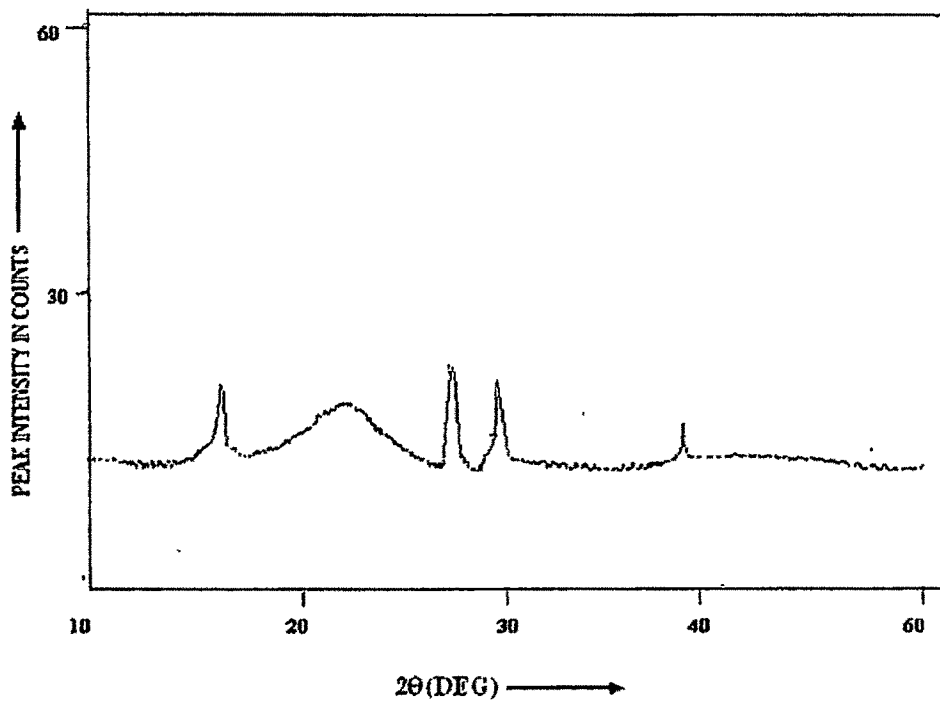


Figure 4.2(c) X-ray diffractogram of quenched sample-B

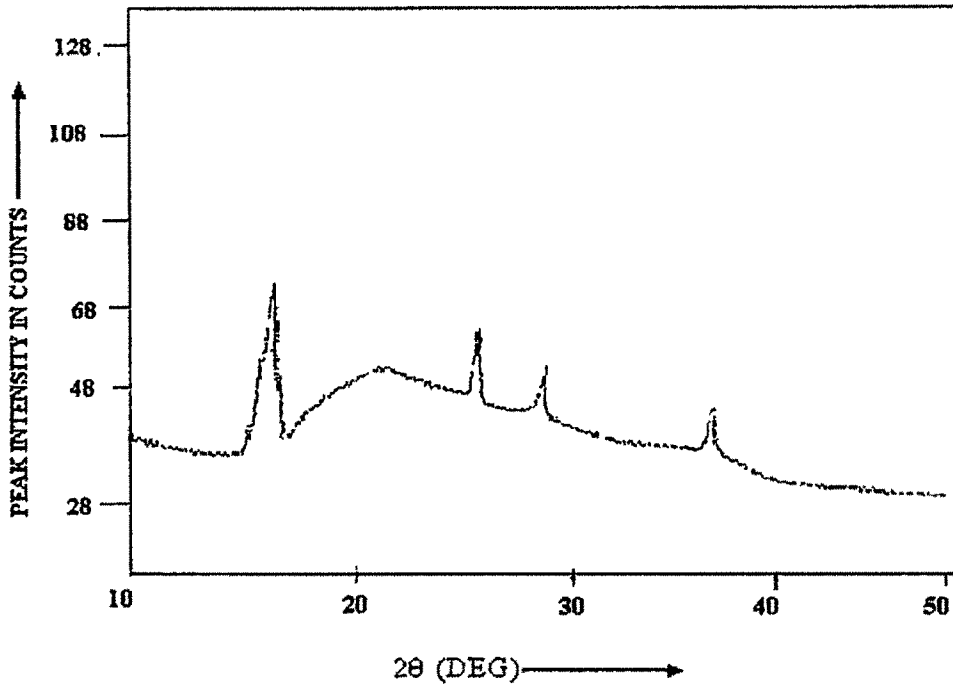


Figure 4.3(a) X-ray diffractogram of unheated sample-C

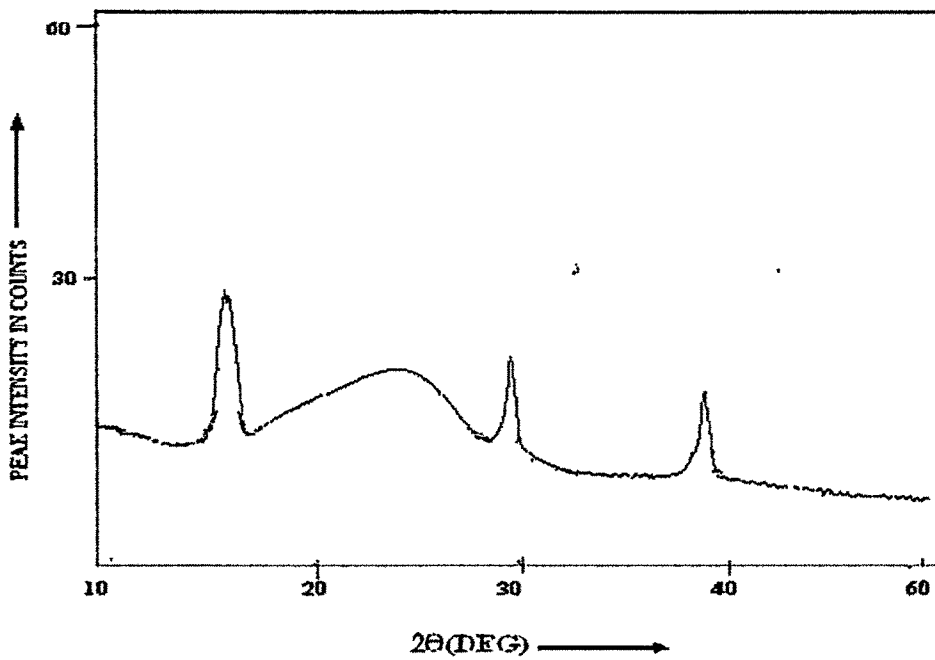


Figure 4.3(b) X-ray diffractogram of annealed sample-C

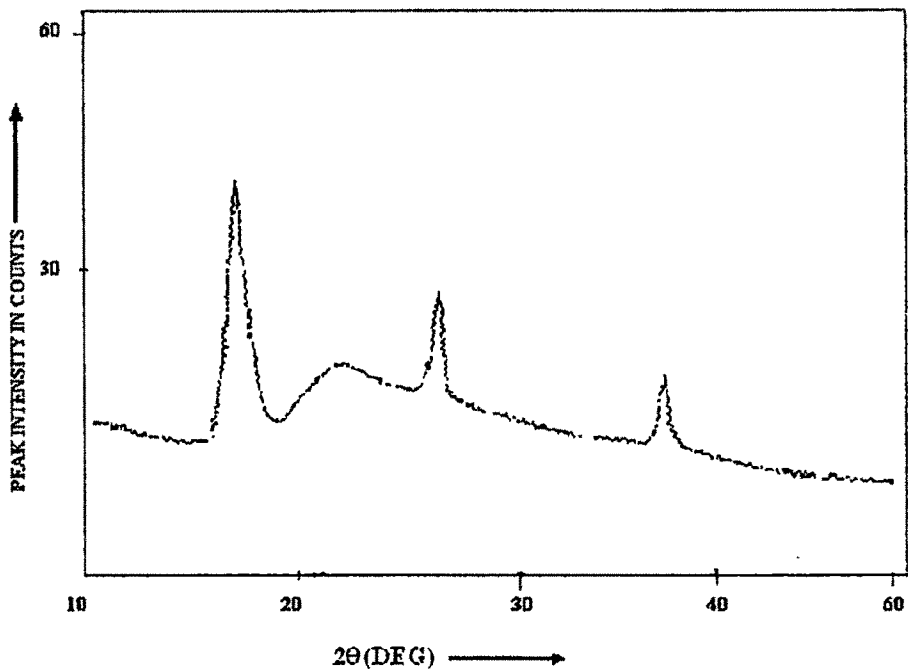


Figure 4.3(c) X-ray diffractogram of quenched sample-C

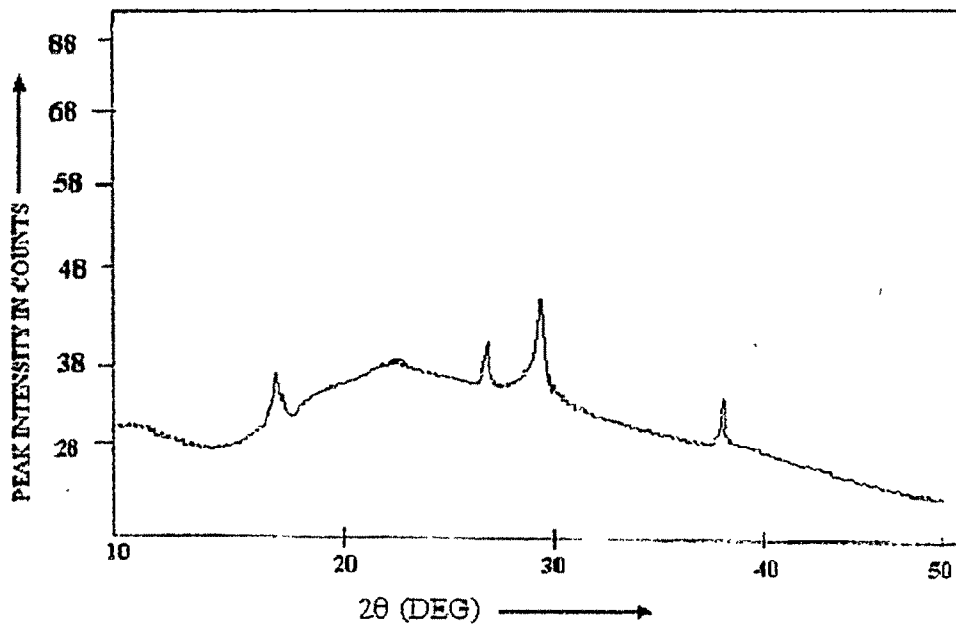


Figure 4.4(a): X-ray diffractogram of unheated sample-D

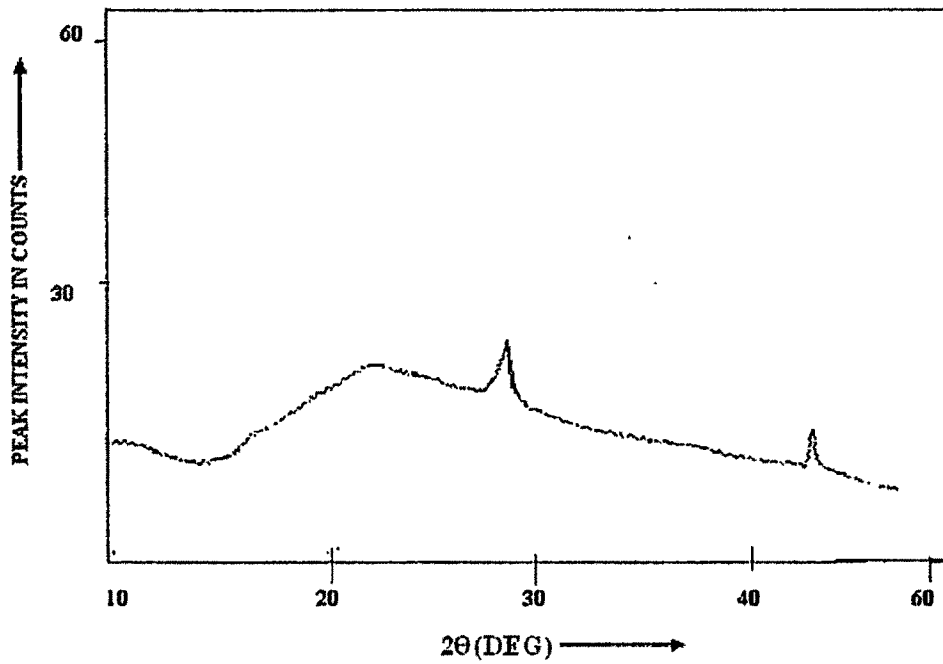


Figure 4.4(b) X-ray diffractogram of annealed sample-D

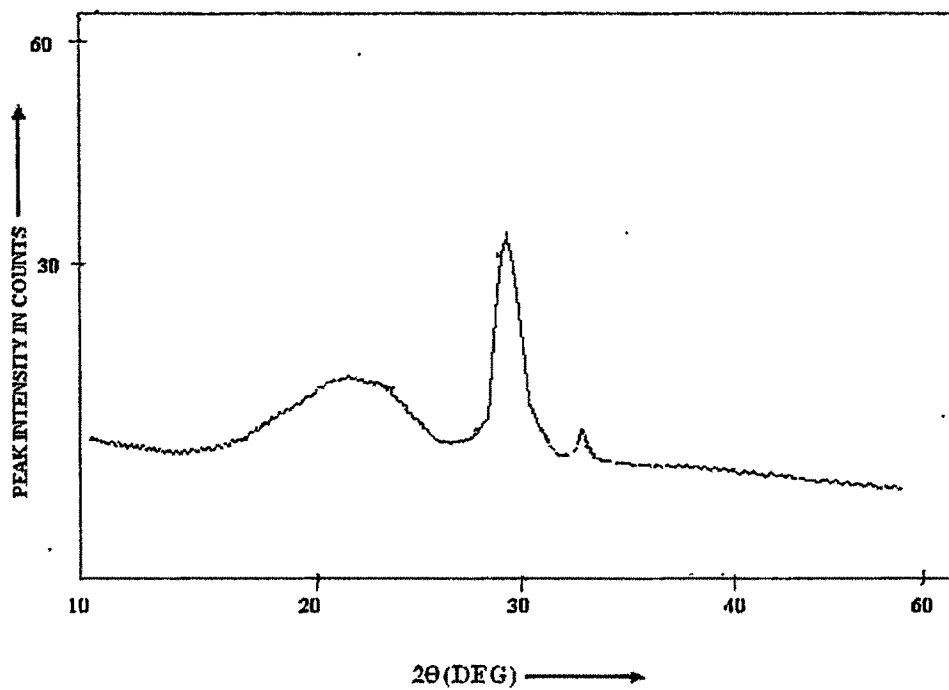


Figure 4.4(c) X-ray diffractogram of quenched sample-D

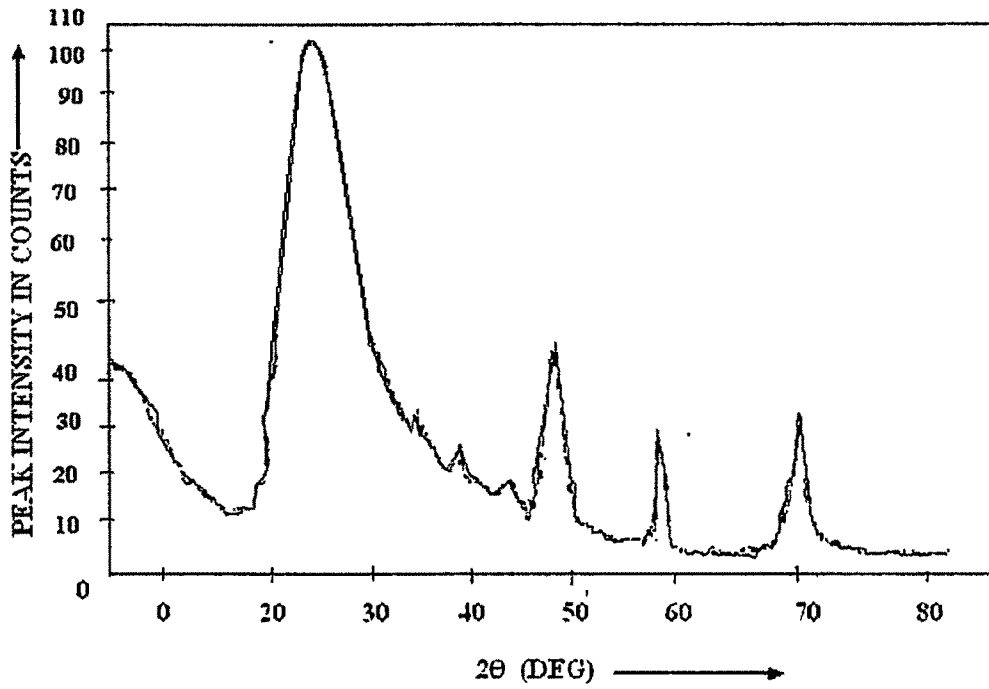


Figure 4.5(a): X-ray diffractogram of unheated sample-E

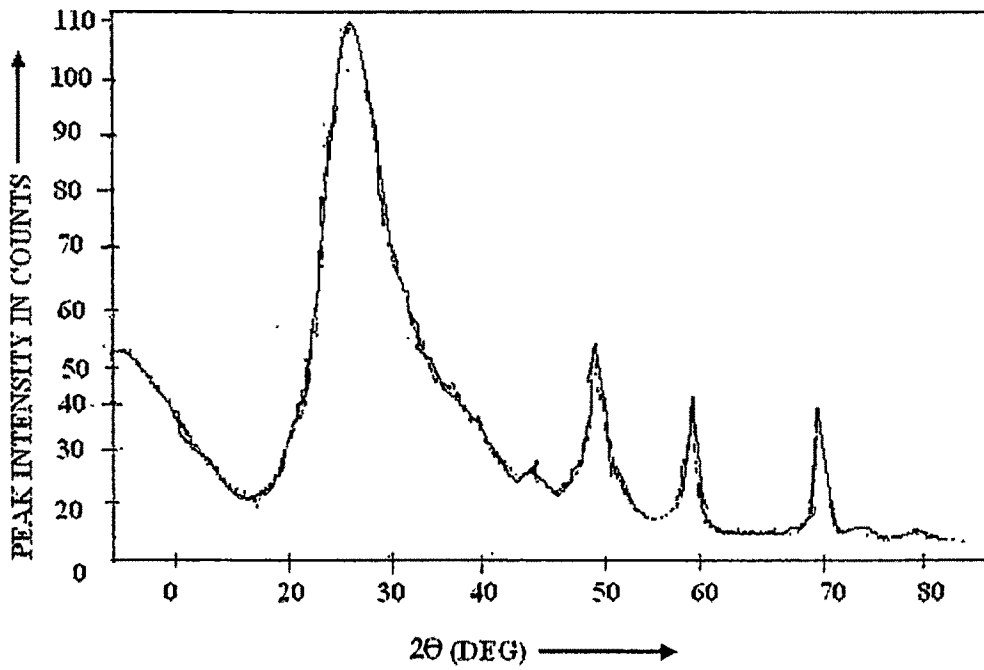


Figure 4.5(b): X-ray diffractogram of annealed sample-E

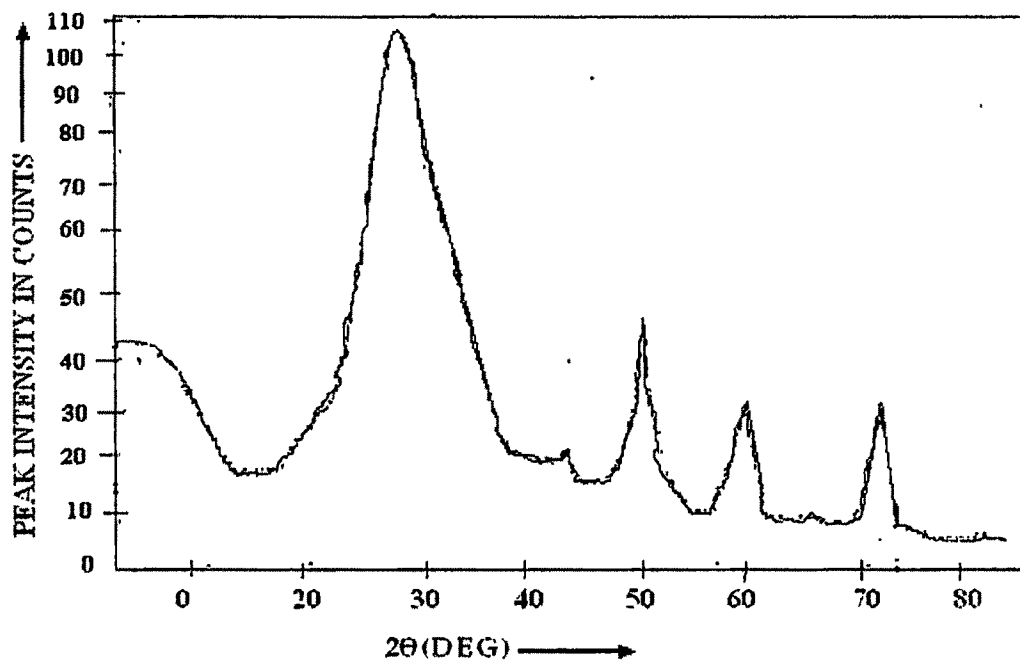


Figure 4.5(c): X-ray diffractogram of quenched sample-E

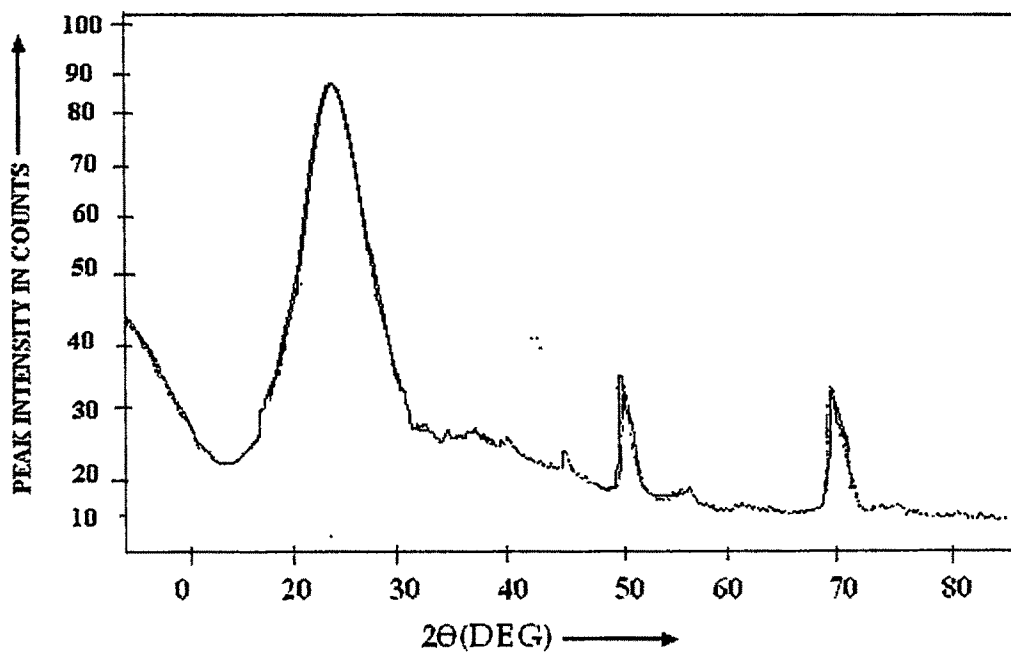


Figure 4.6(a): X-ray diffractogram of unheated sample-F

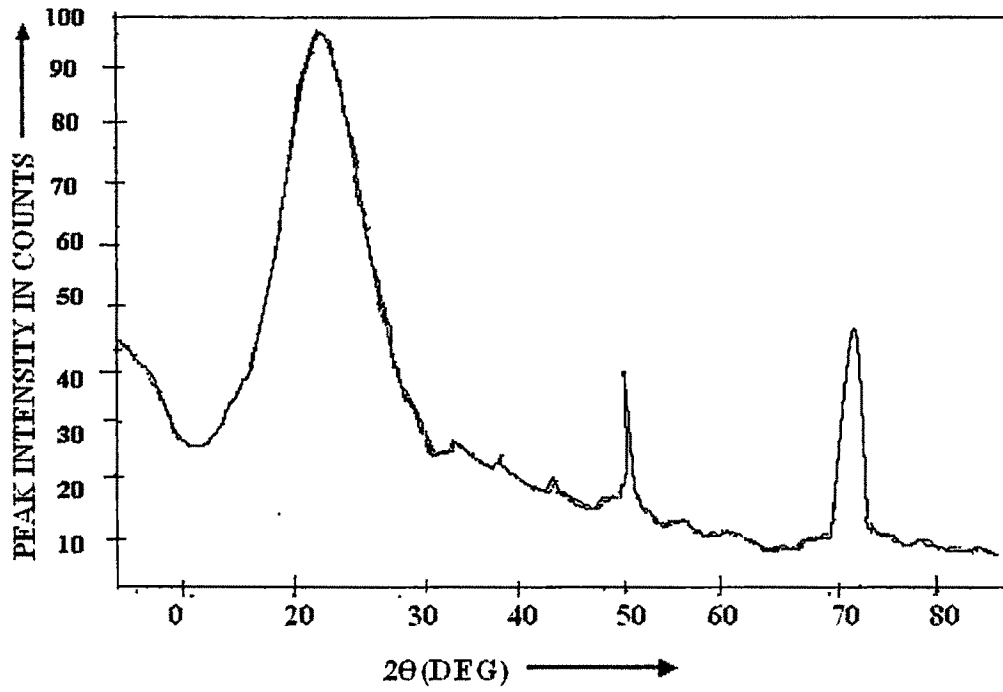


Figure 4.6(b): X-ray diffractogram of annealed sample-F

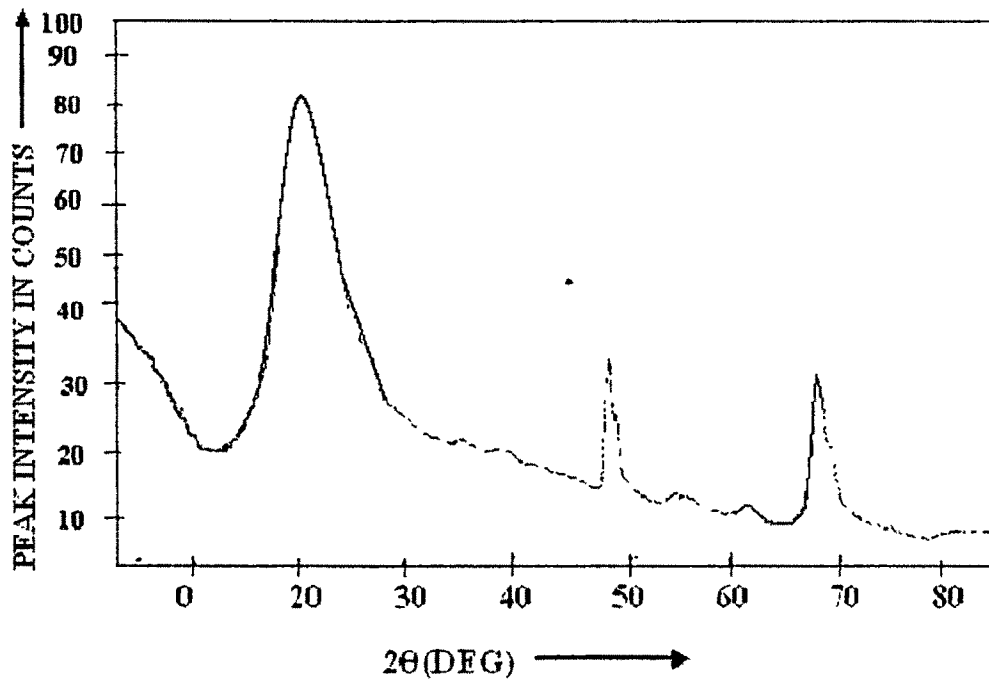


Figure 4.6(c): X-ray diffractogram of quenched sample-F

4.2. X-RAY FLUORESCENCE SPECTROSCOPY STUDY

The X-ray fluorescence(XRF) spectrograms of unheated, and thermally treated (annealed and quenched) leaves of four medicinal plants A: Nephafu (*Clerodendrum colebrookinum*), B: Mahaneem (*Azadirachta indica*), C: Tulsi (*Ocimum sanctum*) and D: Nayantora (*Vinca rosea*) are displayed in figure(4.7,4.8,4.9 and 4.10).Again the XRF spectrogram of unheated and thermally treated(annealed and quenched) fruits E: Bandordima(*Chisocheton paniculatus*) and F: Sarumoin(*Cudrania javanensis*,) are displayed in figure (4.11,4.12,).

The intensity counts in XRF spectrometer technique are recorded for both unheated and thermally treated (annealed and quenched) samples.

From the figure(4.7,4.8,4.9 and 4.10), it has been found that the major elements present in each case of the leaf samples A,B,C & D are Fe (iron), Ca (calcium), and K(potassium) as earlier observation of the plant fibres⁵.

In case of medicinal plant fruits E (figure 4.11) it has been found that the major elements present are Zn (Zinc), Ca (calcium), Fe (iron) and K (potassium). But for the sample F (figure 4.12) it has been found that in addition to those five major elements Rb (Rubidium) is also present.

The relative peak intensities of the leaf samples A, B, C and D corresponding to the K_{α} and K_{β} lines are shown in the table 4.3 and for the fruit samples E and F are shown in the table 4.4. From the table 4.3 it is evident that among the major elements present in each plant leaves, the relative abundance of potassium is found to be more while iron is less. Similarly the relative abundance in case of fruit samples-E potassium was found to be more while iron is less. On the other hand the relative abundance in case of fruit samples F, calcium is found to be more while iron is less.

The intensity counts increase of thermally treated samples. The effect of more in the quenched sample than in annealed sample.

Table 4.3: Intensity counts of medicinal plant leaves recorded in XRF Spectrometer of A-Nephafu, B-Mahaneem, C-Tulsi and D-Nayantora.

Sample	Element present	Intensity in KCPs						XRF records	
		Unheated		Annealed		Quenched		2θ in degree	
		K _β	K _α	K _β	K _α	K _β	K _α	For k _β	For k _α
A	Fe	3.1	19.8	3.8	20.2	4.0	24.3	51.1	57.6
	Ca	40.2	364.1	42.1	369.2	47.2	394.2	100.2	113.2
	K	59.3	485.3	61.2	490.8	67.6	504.8	118.2	138.1
B	Fe	3.9	20.2	4.2	22.8	4.8	29.3	59.1	64.7
	Ca	49.3	382.1	51.1	387.1	60.2	49.2	100.4	114.3
	K	16.6	490.2	63.2	498.3	70.3	508.2	119.2	139.2
C	Fe	7.2	32.8	8.4	36.2	12.0	42.3	52.1	58.0
	Ca	53.8	399.2	56.2	408.8	63.8	428.2	101.0	115.2
	K	72.0	520.3	80.2	528.3	92.3	543.8	122.0	140.1
D	Fe	6.3	35.1	9.3	42.0	13.0	49.3	58.7	62.1
	Ca	55.5	401.5	57.7	415	69.2	456.5	115.0	125.2
	K	69.0	590.0	83.1	595	98.5	597.1	130.1	152.3

Table 4.4: Intensity counts of medicinal plants fruits recorded in XRF Spectrometer for
E-Bandordima and F-Sarumion

Sample	Element present	Intensity in KCPS						XRF records	
		Unheated		Annealed		Quenched		2θ in degree	
		Kβ	Kα	Kβ	Kα	Kβ	Kα	For Kβ	For Kα
E	Zn	10.1	21.8	11.7	26.6	12.1	26.5	44.3	51.1
	Fe	7.5	25.5	8.7	27.2	9.1	27.5	67.2	73.2
	Ca	18.2	40.1	19.2	43.5	20.4	44.3	105.6	116.2
	K	23.1	78.5	24.3	81.4	24.3	82.1	131.5	142.3
F	Rb	6.3	20.4	7.1	22.8	7.6	24.3	24.5	32.1
	Zn	7.2	17.5	8.3	18.5	8.1	19.2	52.2	60.3
	Fe	1.5	5.6	2.3	6.5	2.7	7.2	82.1	89.5
	Ca	3.2	20.4	3.9	21.3	4.1	22.1	111.3	117.5
	K	7.5	80.2	8.2	81.3	8.5	82.4	131.2	139.3

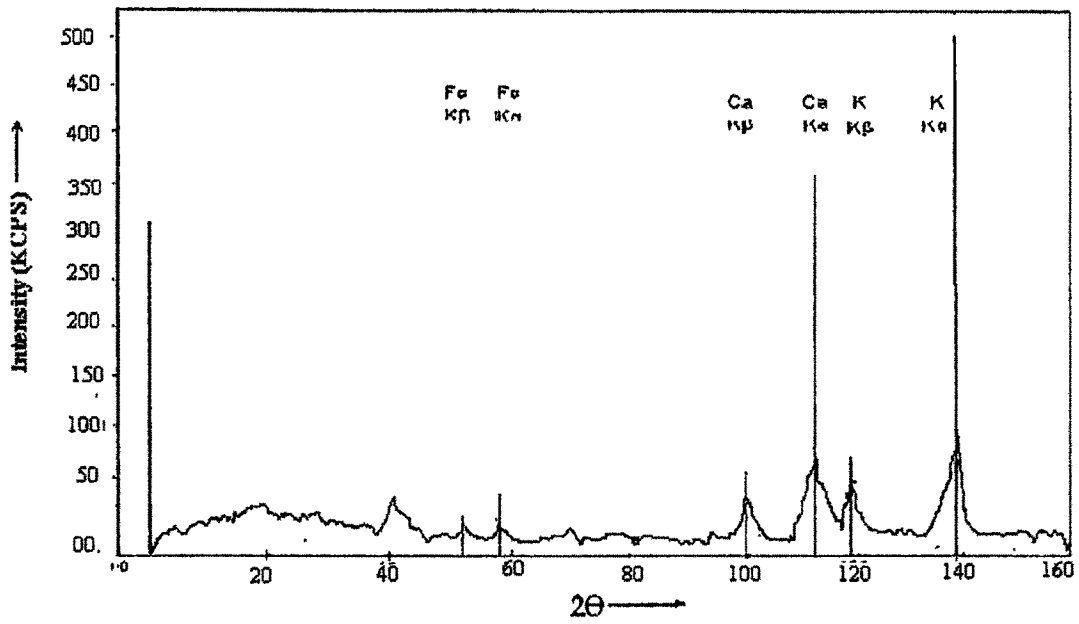


Figure 4.7(a): The X-ray fluorescence (XRF) spectrograms of unheated sample A

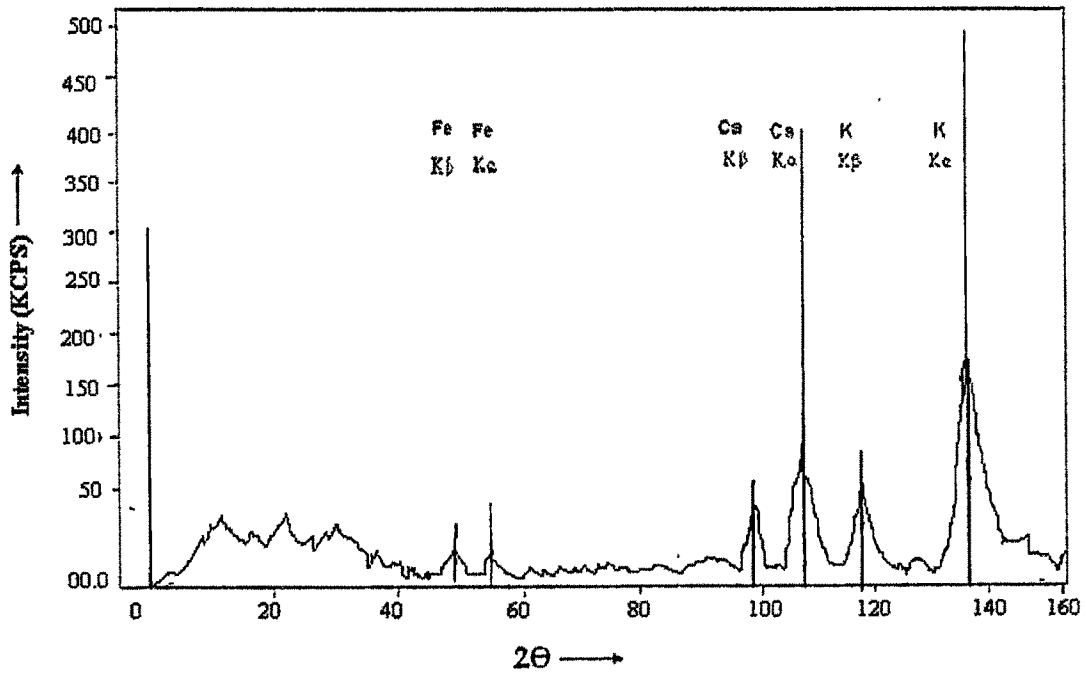
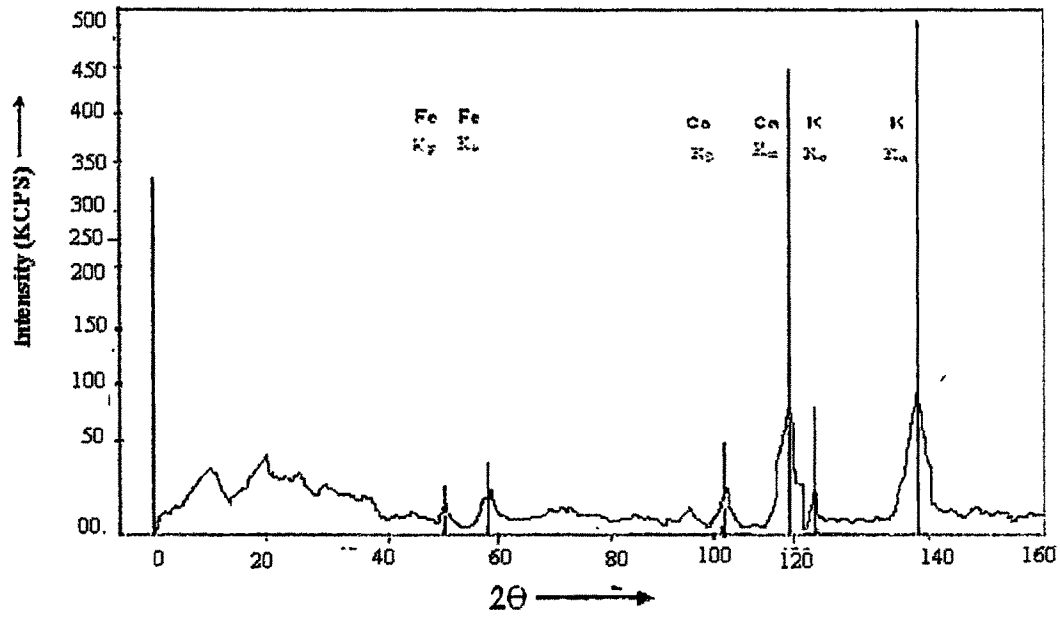


Figure 4.7(b): The X-ray fluorescence (XRF) spectrograms of annealed sample A



4.7 (c): The X-ray fluorescence (XRF) spectrograms of quenched sample A

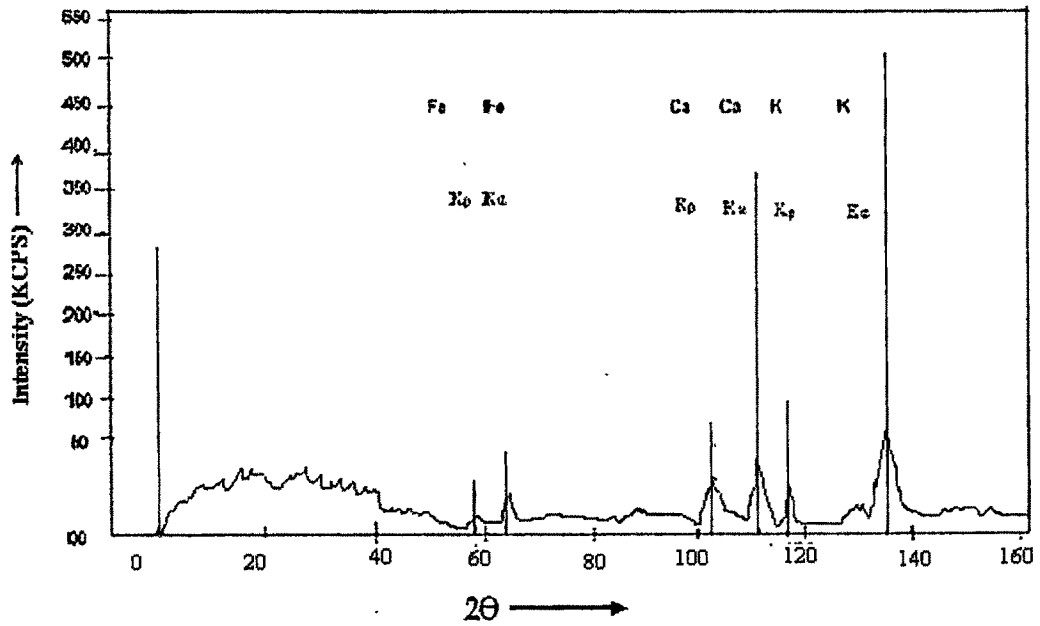


Figure 4.8(a): The X-ray fluorescence (XRF) spectrograms of unheated sample B

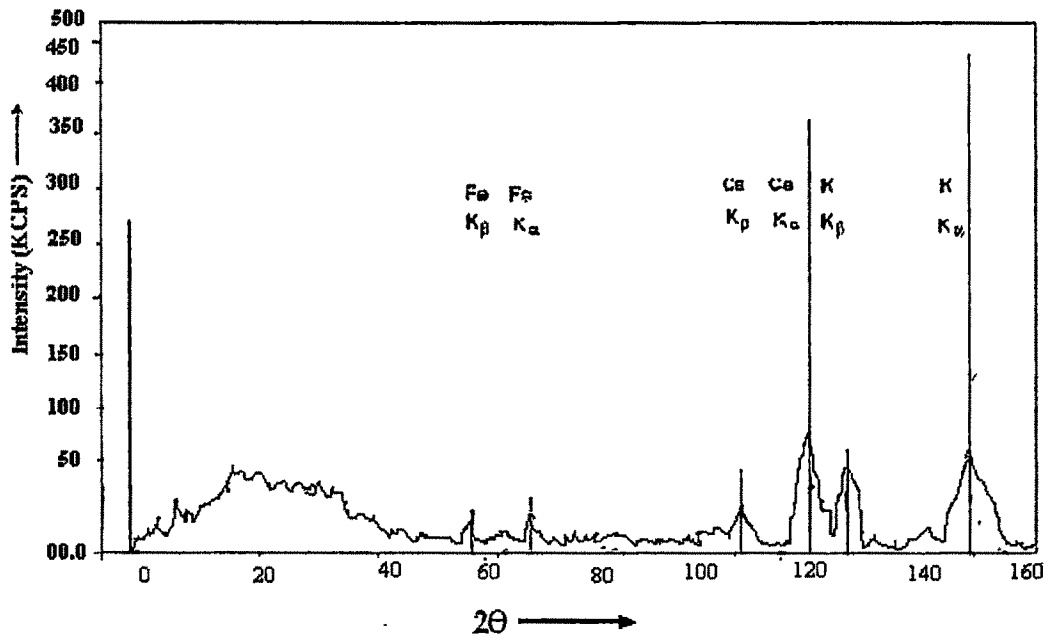


Figure 4.8(b): The X-ray fluorescence (XRF) spectrograms of annealed sample B

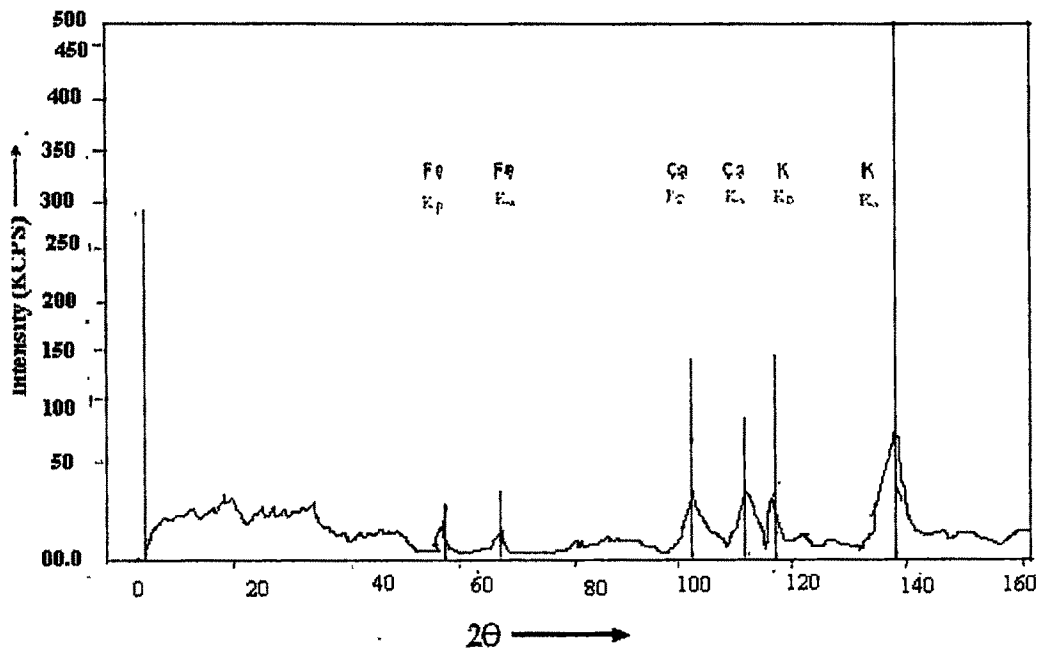


Figure 4.8(c): The X-ray fluorescence (XRF) spectrograms of quenched Sample B

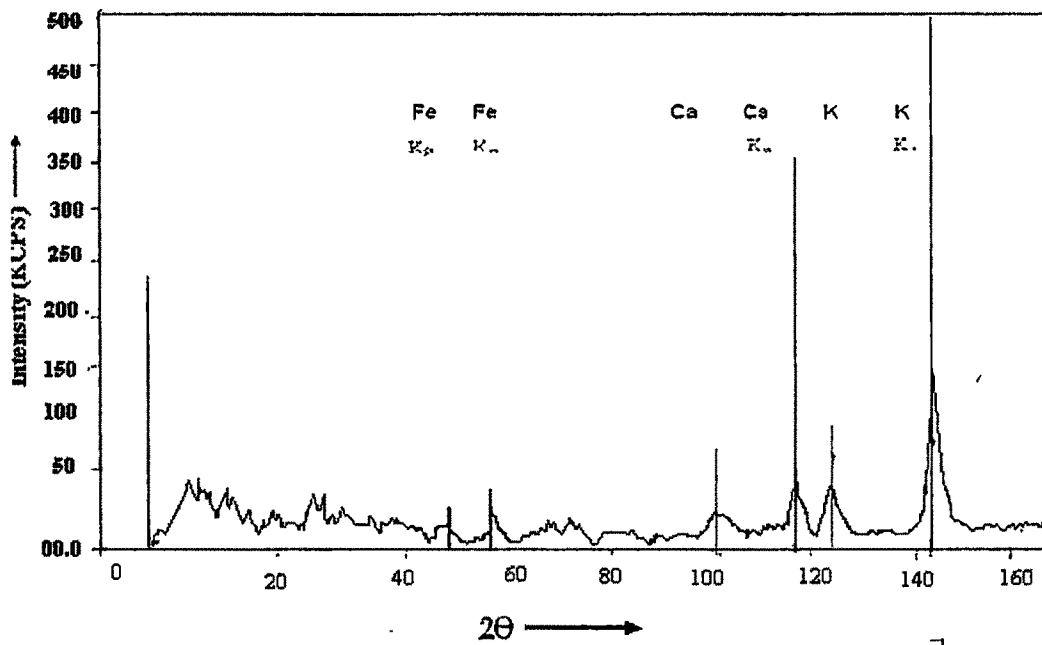


Figure 4.9(a): The X-ray fluorescence (XRF) spectrograms of unheated sample C

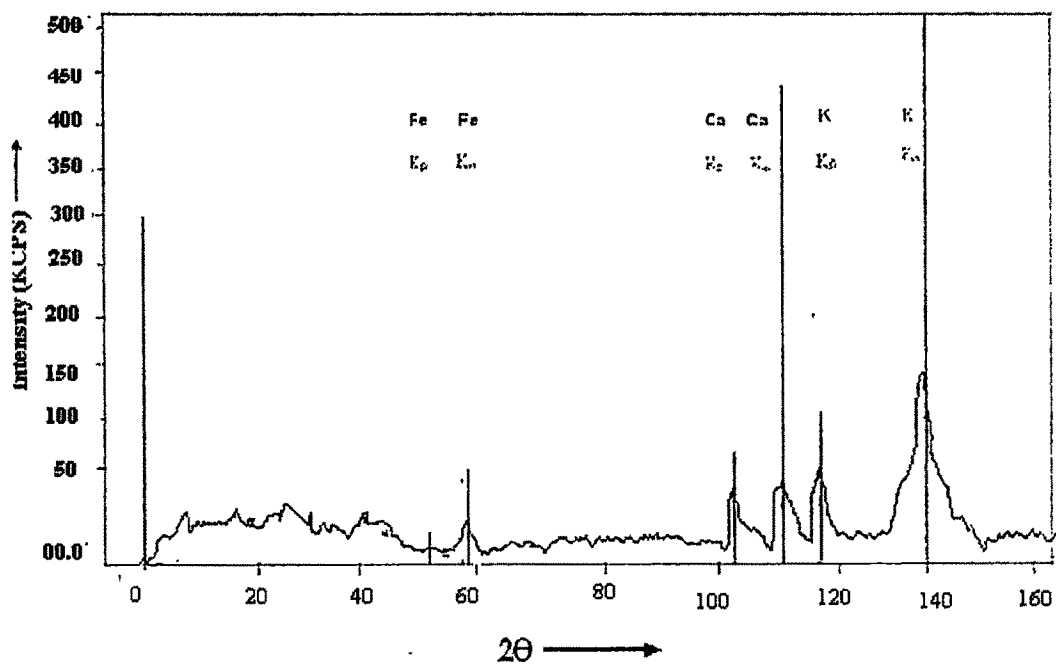


Figure 4.9(b): The X-ray fluorescence (XRF) spectrograms of annealed Sample C

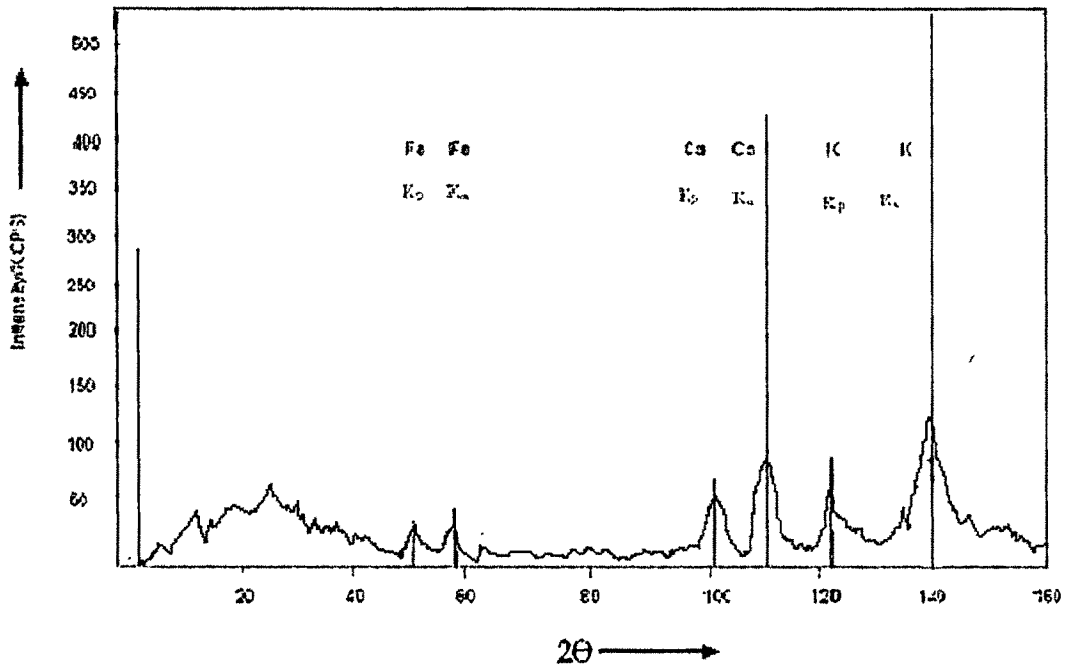


Figure 4.9(c): The X-ray fluorescence (XRF) spectrograms of quenched sample C

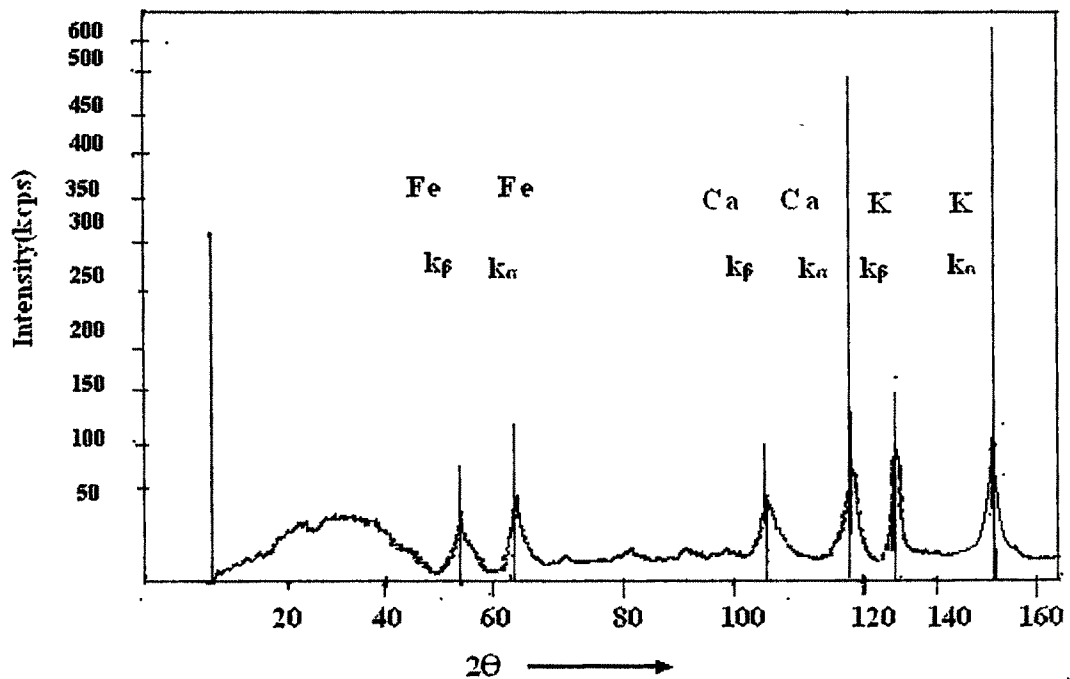


Figure 4.10(a): The X-ray fluorescence (XRF) spectrograms of unheated sample D

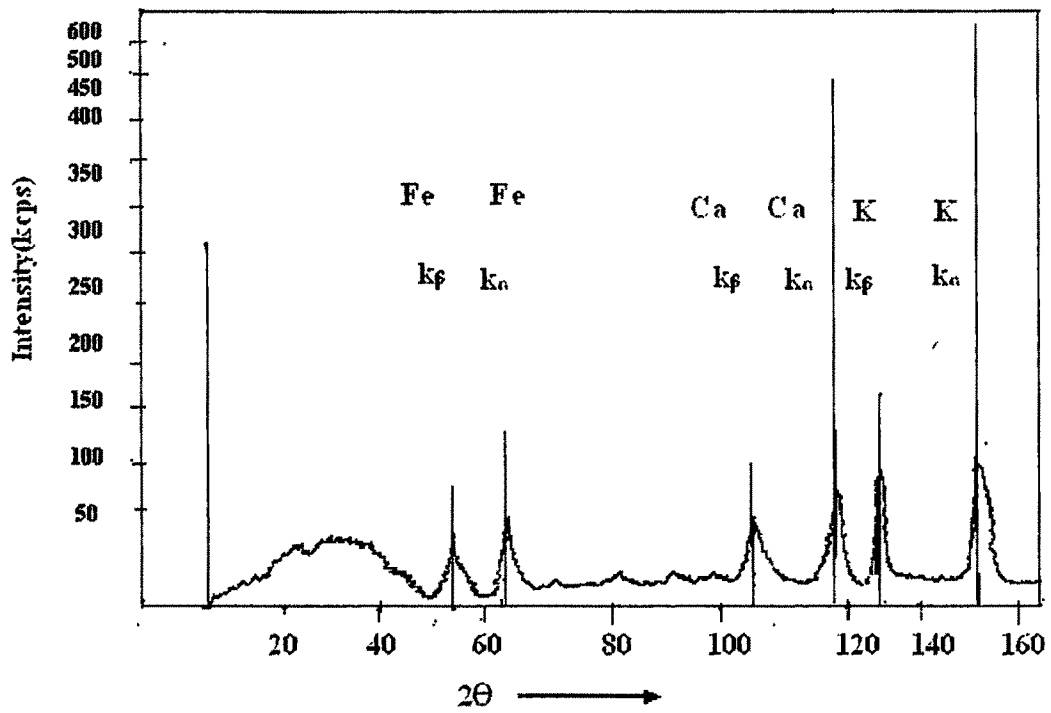


Figure 4.10(b): The X-ray fluorescence (XRF) spectrograms of annealed sample-D

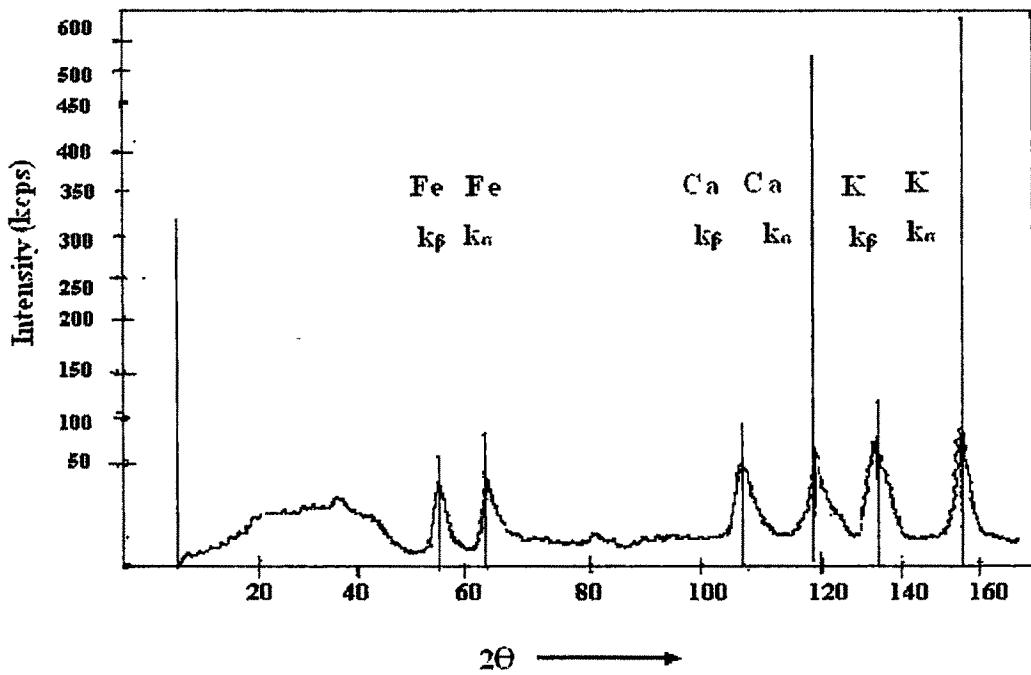


Figure 4.10(c): The X-ray fluorescence (XRF) spectrograms of quenched sample-D

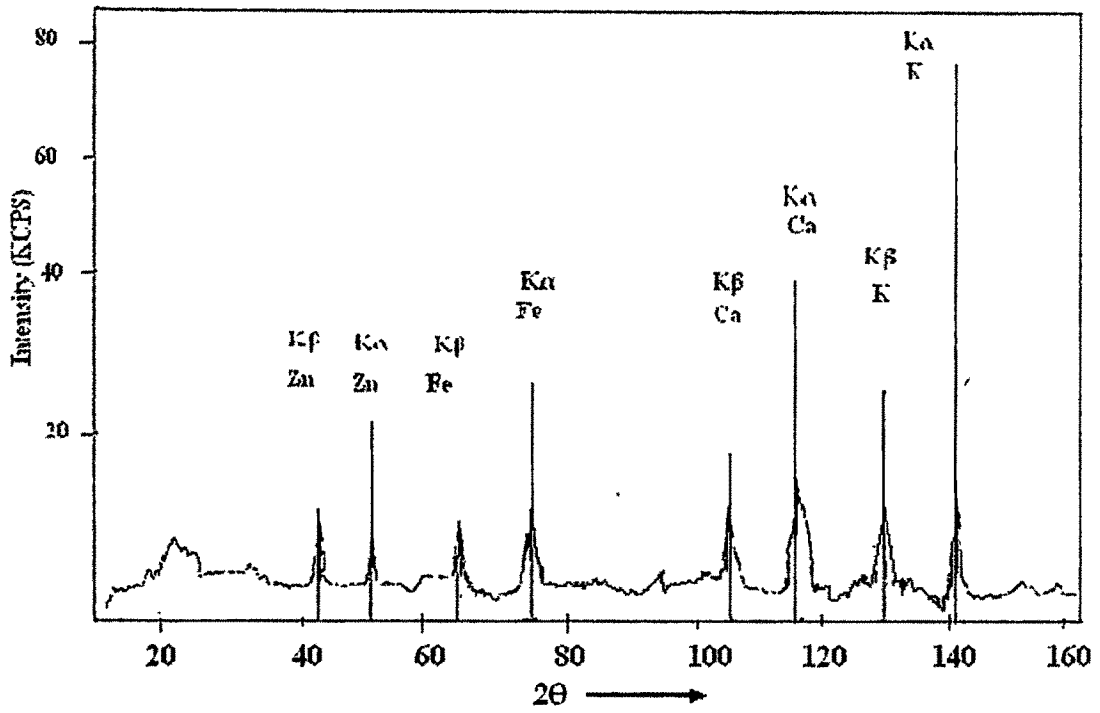


Figure 4.11(a): The X-ray fluorescence (XRF) spectrograms of unheated sample-E

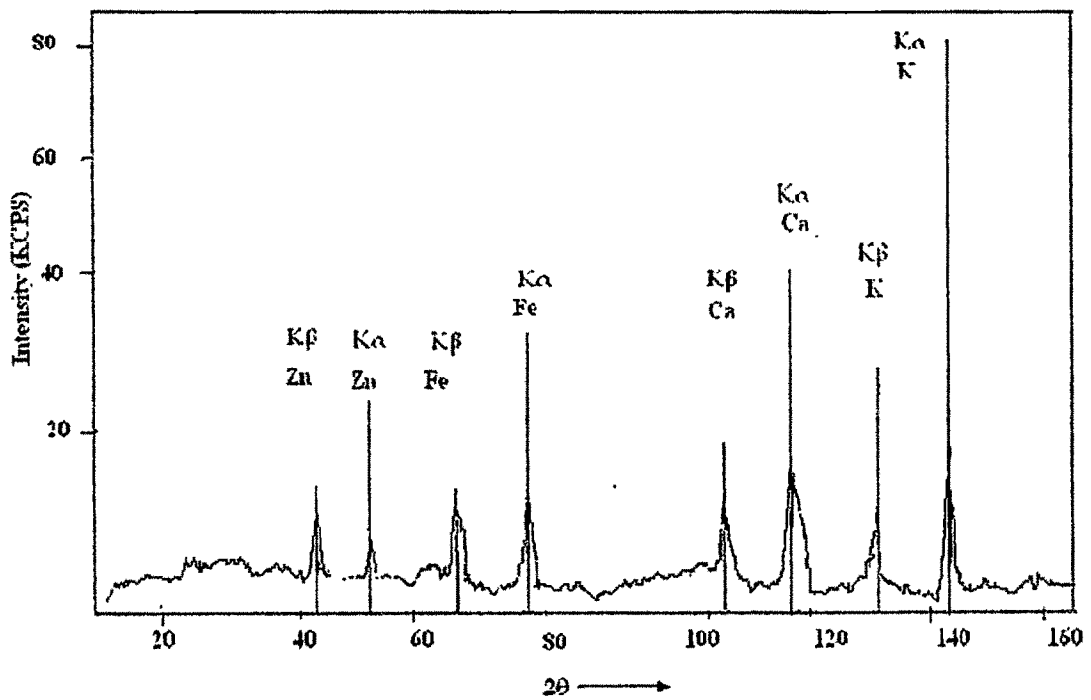


Figure 4.11(b): The X-ray fluorescence (XRF) spectrograms of annealed sample-E

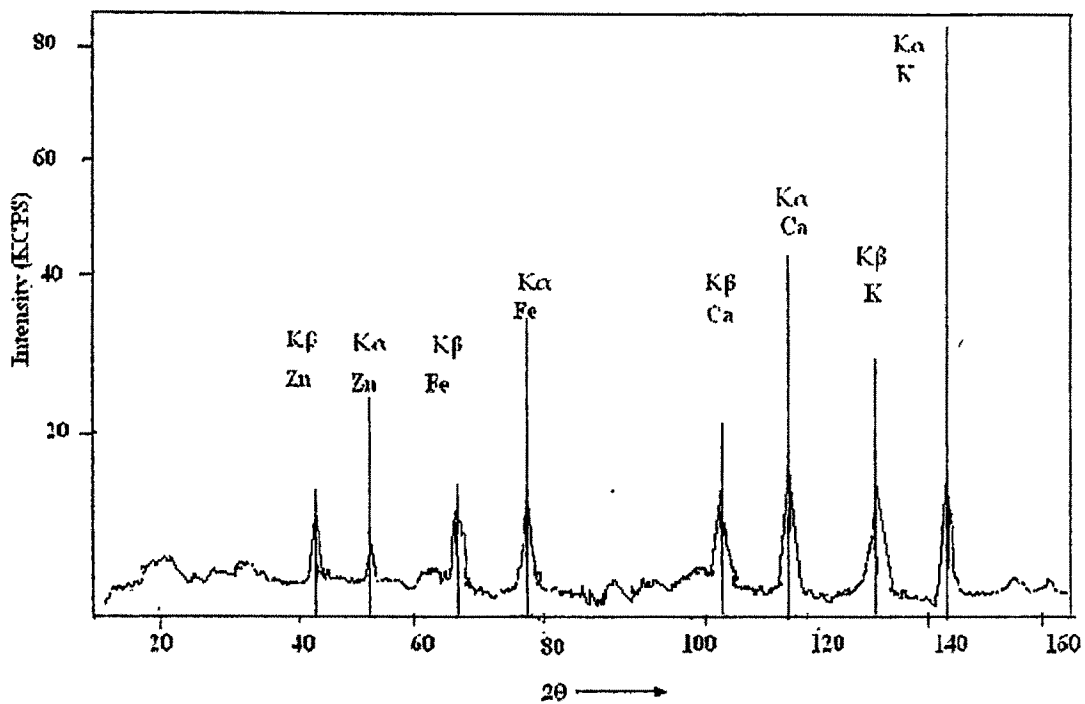


Figure 4.11(c): The X-ray fluorescence (XRF) spectrograms of quenched sample-E

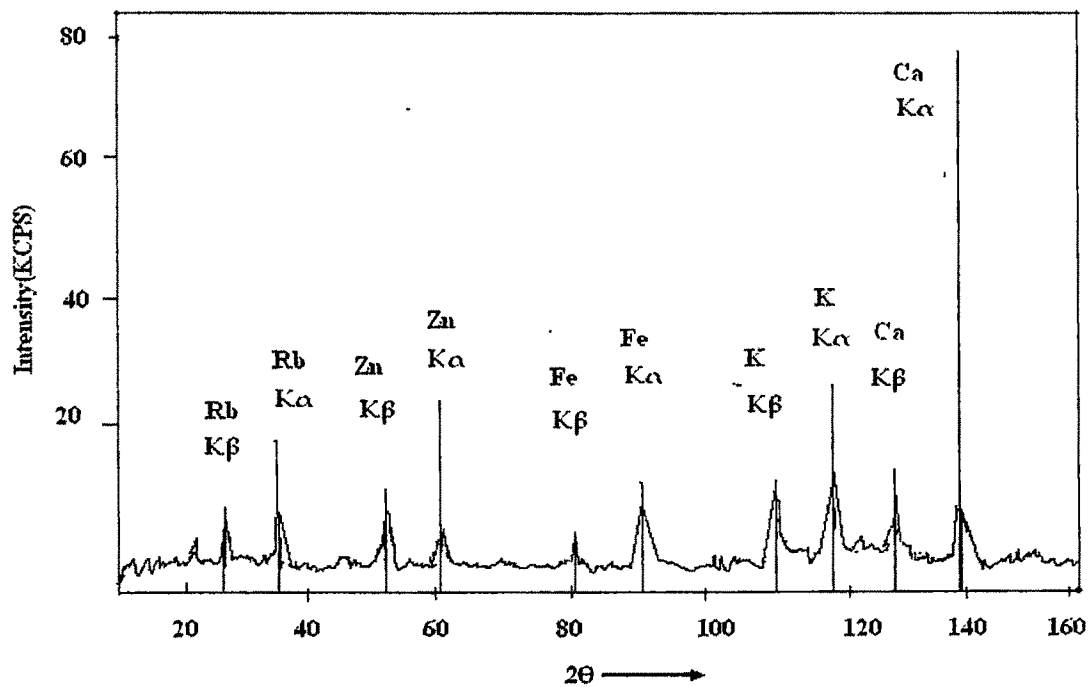


Figure 4.12(a): The X-ray fluorescence (XRF) spectrograms of unheated sample-F

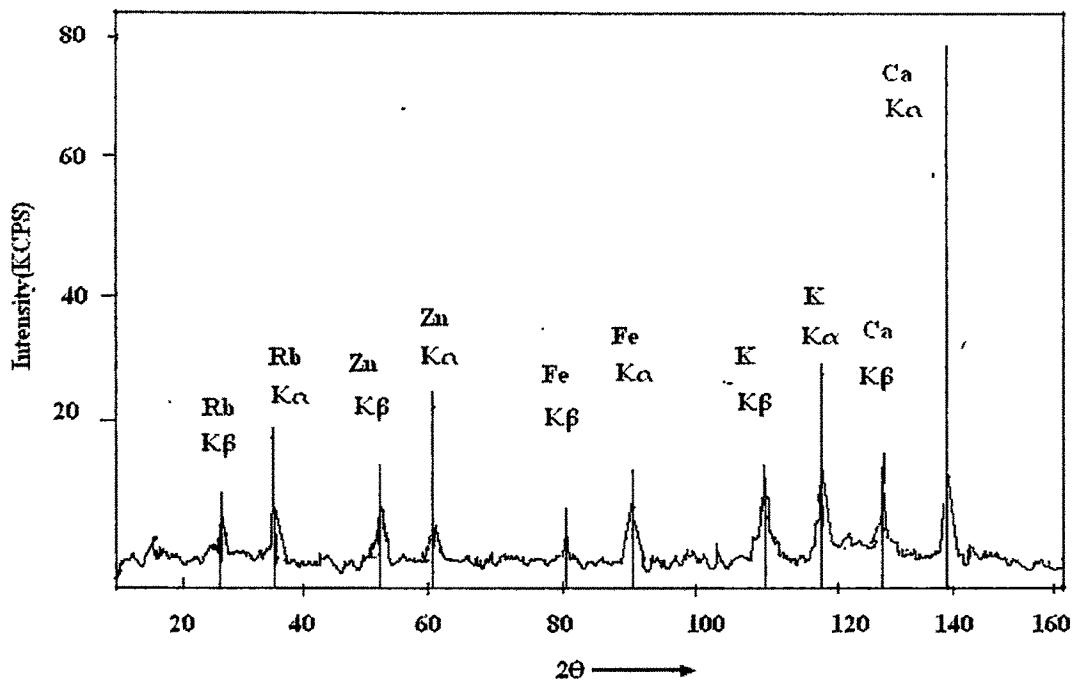


Figure 4.12(b): The X-ray fluorescence (XRF) spectrograms of annealed sample F

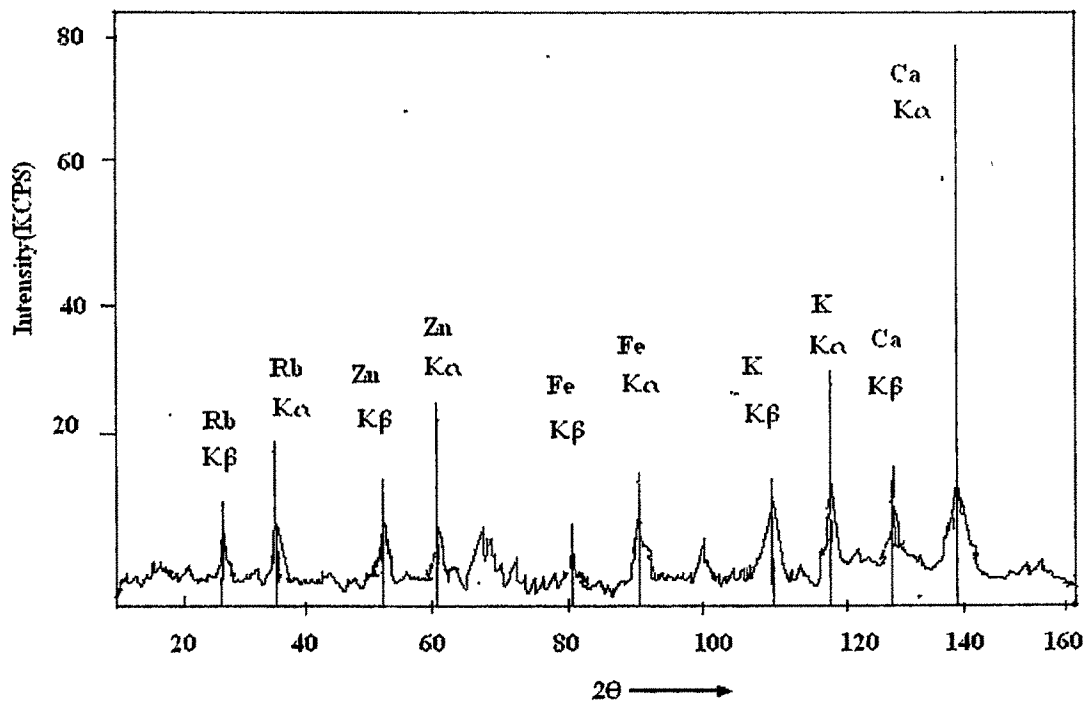


Figure 4.12(c): The X-ray fluorescence (XRF) spectrograms of quenched sample F

4.3. STUDY OF THERMAL DECOMPOSITION OF MEDICINAL PLANT

LEAVES AND FRUITS SAMPLE USING TG, DTG AND DSC

TECHNIQUES

Study of thermal stabilities of the leave samples A: Nephafu (*Clerodendron colebrookimum*), B: Mahaneem (*Azadirachta indica*), C: Tulsi (*Ocimum sanctum*) and D: Nayantora (*Vinca rosea*); fruit samples E: Bandordima (*Chisocheton paniculatus*) and F: Sarumoin (*Cudrania javanensis*,) are carried out by using thermogravimetric (TG) and derivative thermogravimetric (DTG) methods. Thermogravimetric studies for each sample are performed independently in air as well as in the presence of oxygen to differentiate the arial oxidation and oxidation with oxygen of the medicinal plant leaves and fruits on heating. Thermograms for the samples are also recorded in nitrogen atmospheres to see the effect of thermal decomposition under anaerobic condition. The DSC of each sample at air atmosphere is recorded to obtain the thermodynamic parameters such as activation energy (E_1),) and change of entropy (ΔS).The activation energy (E_1) corresponding to thermal decomposition at various stages are calculated from respective TG curves by using Feeman and Carroll equation.

The thermogravimetric (TG) & DTG profiling for the leave samples A, B, C & D and also fruit samples E & F are shown in figures 4.13, 4.15, 4.17, 4.19, 4.21 and 4.23 in air, oxygen and nitrogen atmosphere respectively. Differential of each of the weight loss profiles are also drawn in the figures. The differentials enable to determine the temperature at which the weigh loss takes place. In each figure, there are three parts a, b and c representing the thermograms of the samples in air, oxygen and nitrogen respectively.

In figure 4.13, 4.15, 4.17, 4.19, 4.21 and 4.23, it is evident that the all samples have similar tendency to degrade under thermal treatments, however there is minute differences in the temperature ranges where the thermal decompositions are taken place.

Differential Thermal Analysis (DTA) curves of air, oxygen and nitrogen at heating rate 10K/min are displayed for the sample A, B, C, D, E and F in figure 4.14, 4.16, 4.18, 4.20, 4.22 and 4.24 respectively. Each of the DTA thermogram shows one endothermic and one exothermic change in certain temperature ranges. These are also reflected in the heat flow vs. temperatures Differential Scanning Calorimetry(DSC) profiles for the all samples and the DSC profile in air for the medicinal plant leave samples A, B, C & D; fruit samples E & F are shown in figures 4.25, 4.26, 4.27, 4.28, 4.29 and 4.30 respectively. This obvious reason for similar trends in each case can be attributed to the analogous structural pattern being present in the back bone of the leaves and fruits⁶

Again in the DSC profiling heat flow vs. temperatures for the six samples A, B, C, D, E and F shows degradation tendency. In the temperature range from 300 to 685K all thermograms shows three distinct stages of decomposition with sharp weight loss. The thermal behaviors of each sample at this temperature interval in air, oxygen and nitrogen atmosphere are discussed by fragmenting the TG graphs. This simplification is made in accordance with the earlier discussion that there is three distinct sets of thermal process occur in each case. For understanding the TG shown in figure 4.13(a) there are three segments which are denoted as S₁, S₂ and S₃ in figure. The following are the independent discussions on each of these three segments.

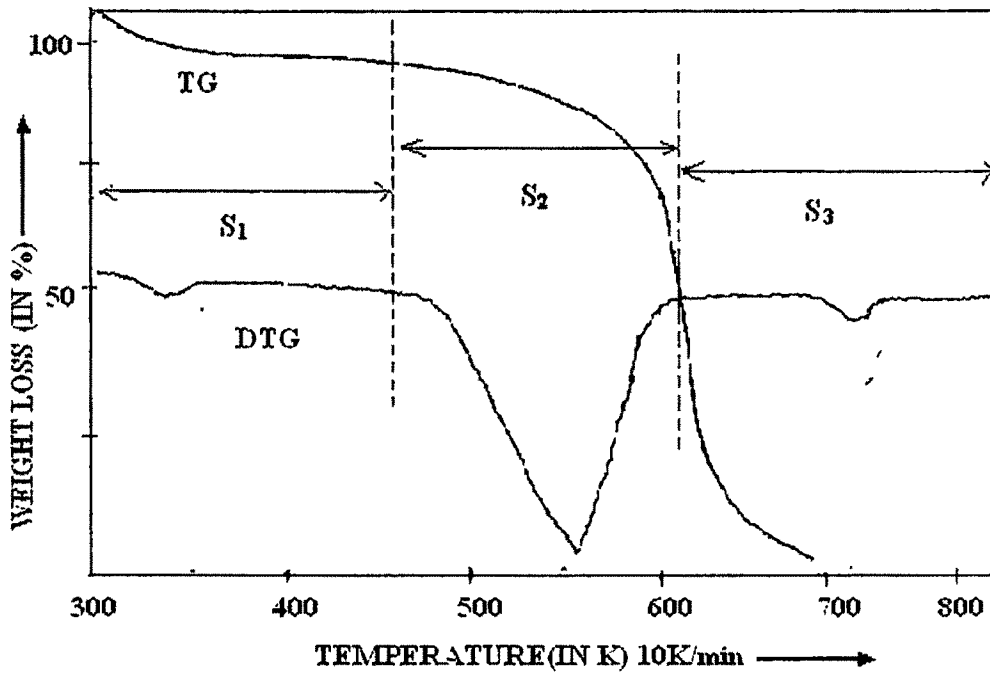


Figure 4.13(a): TG and DTG Thermograms of Sample -A in air atmosphere

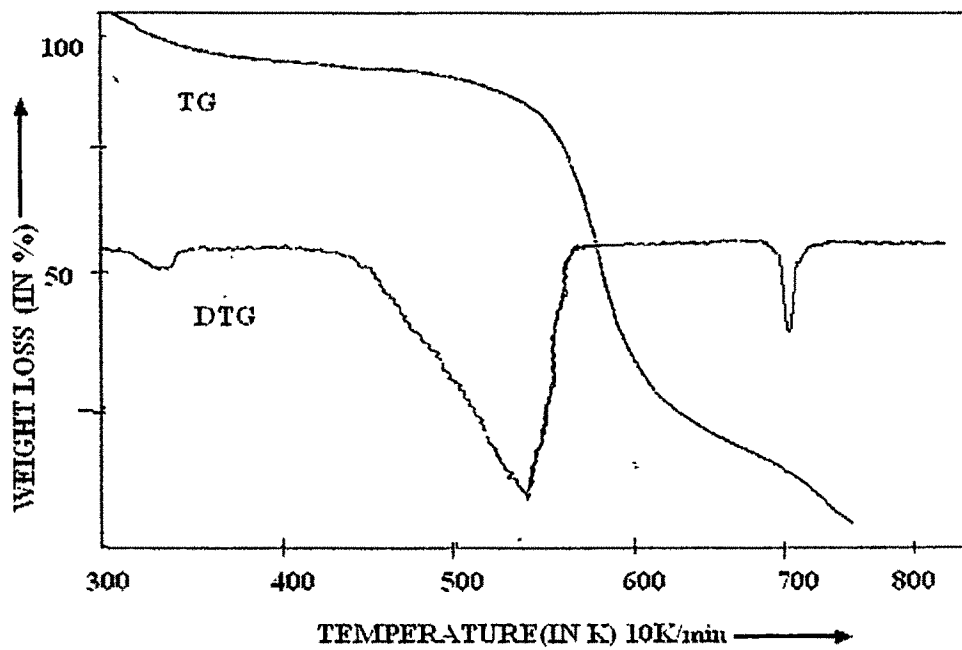


Figure 4.13(b): TG and DTG Thermograms of Sample-A in oxygen atmosphere

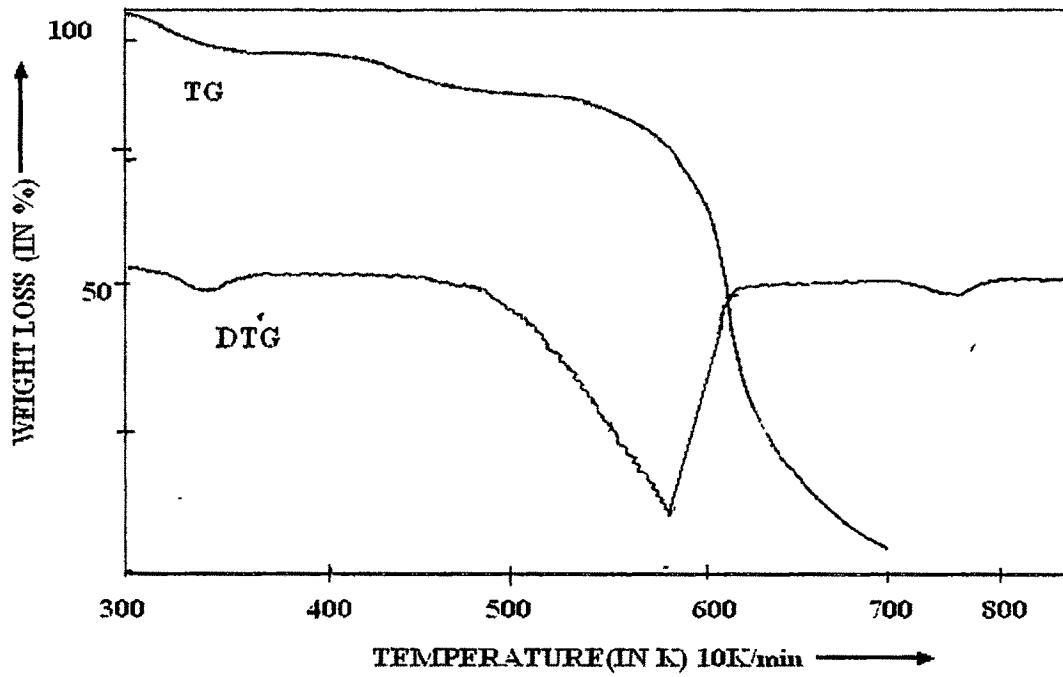


Figure 4.13(c): TG and DTG Thermograms of Sample -A in nitrogen atmosphere

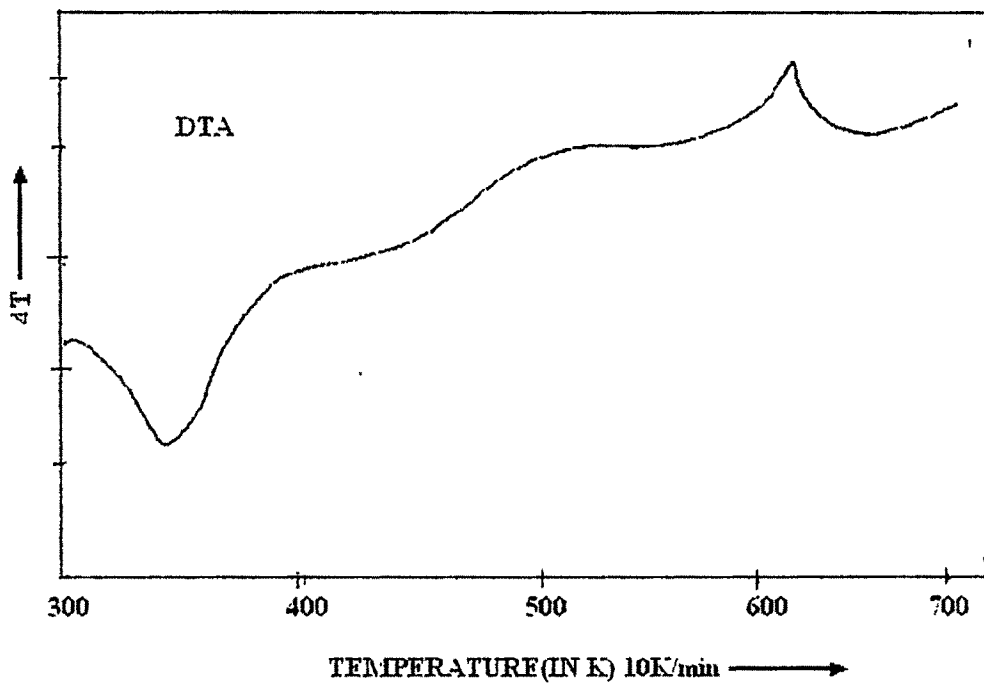


Figure 4.14(a): DTA Thermograms of Sample-A in air atmosphere

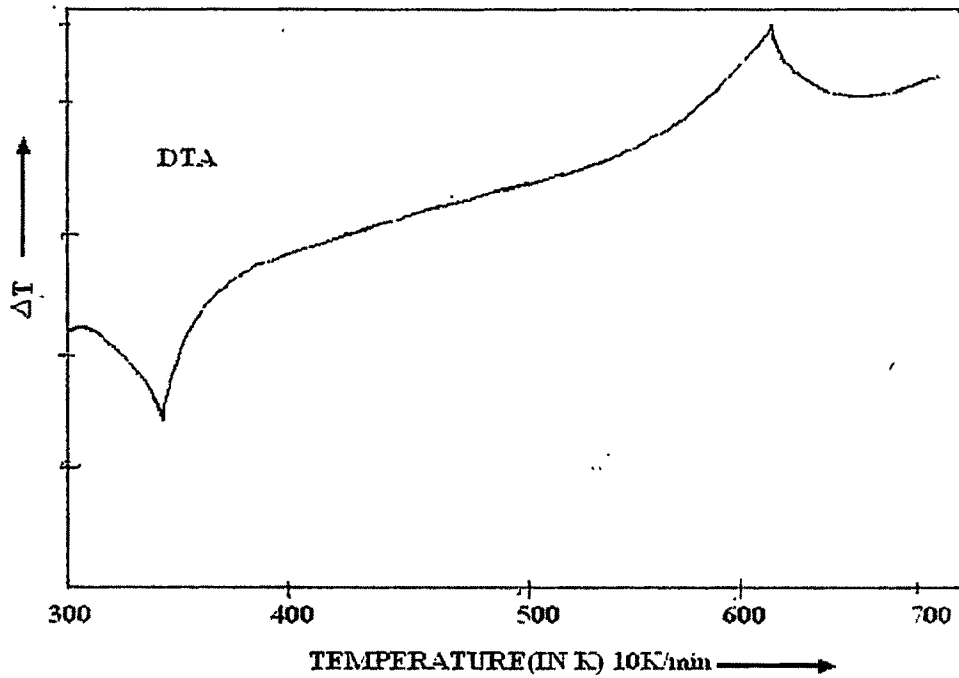


Figure 4.14(b): DTA Thermograms of Sample-A in oxygen atmosphere

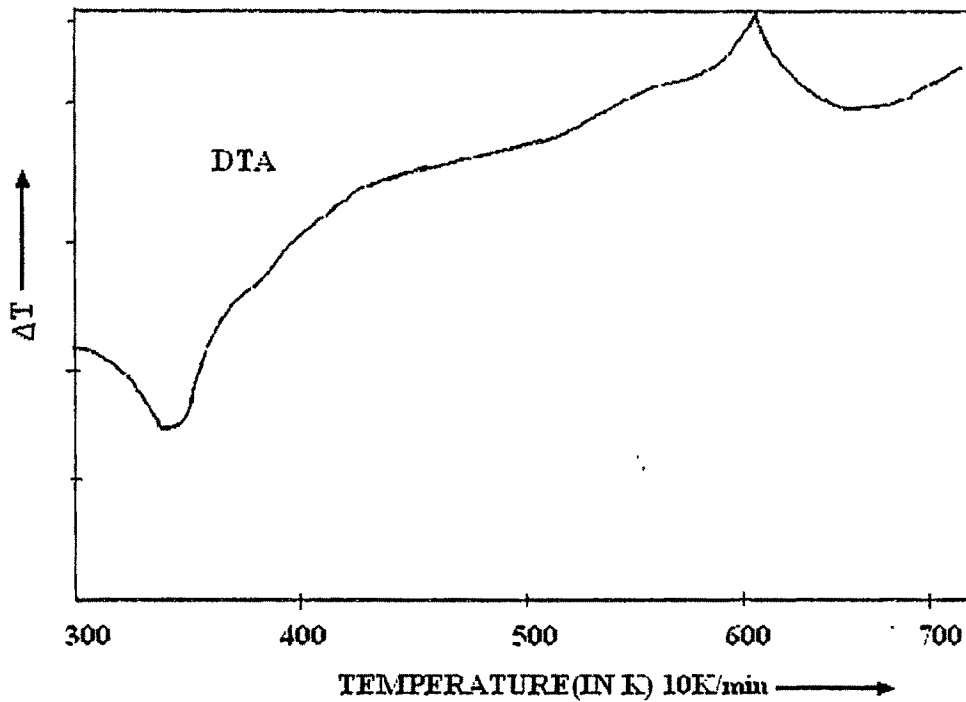


Figure 4.14(c): DTA Thermograms of Sample -A in nitrogen atmosphere

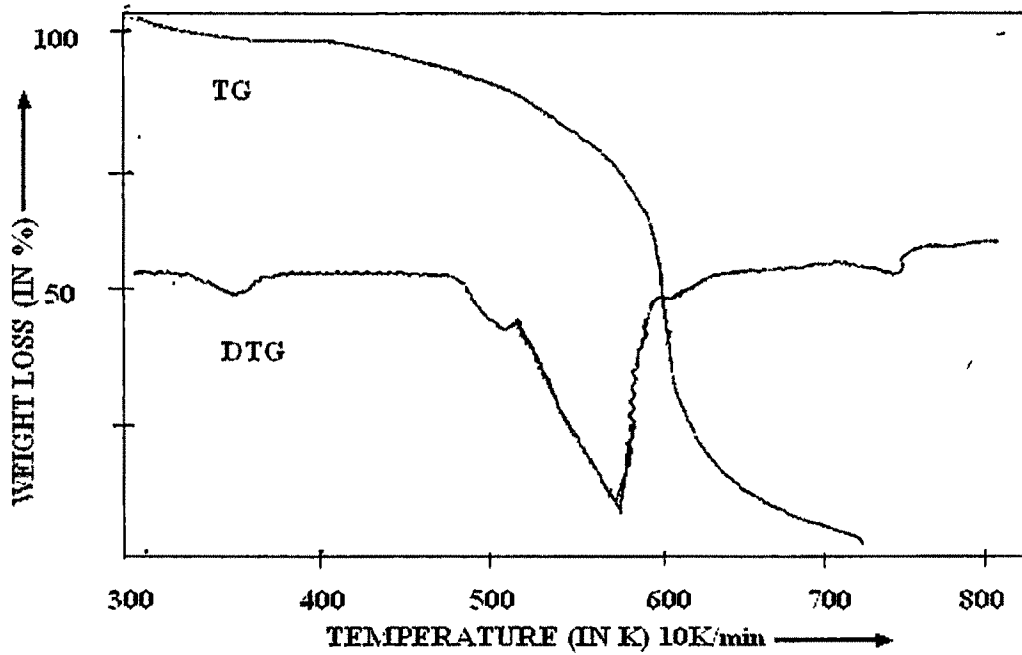


Figure 4.15(a): TG and DTG Thermograms of Sample-B in air atmosphere

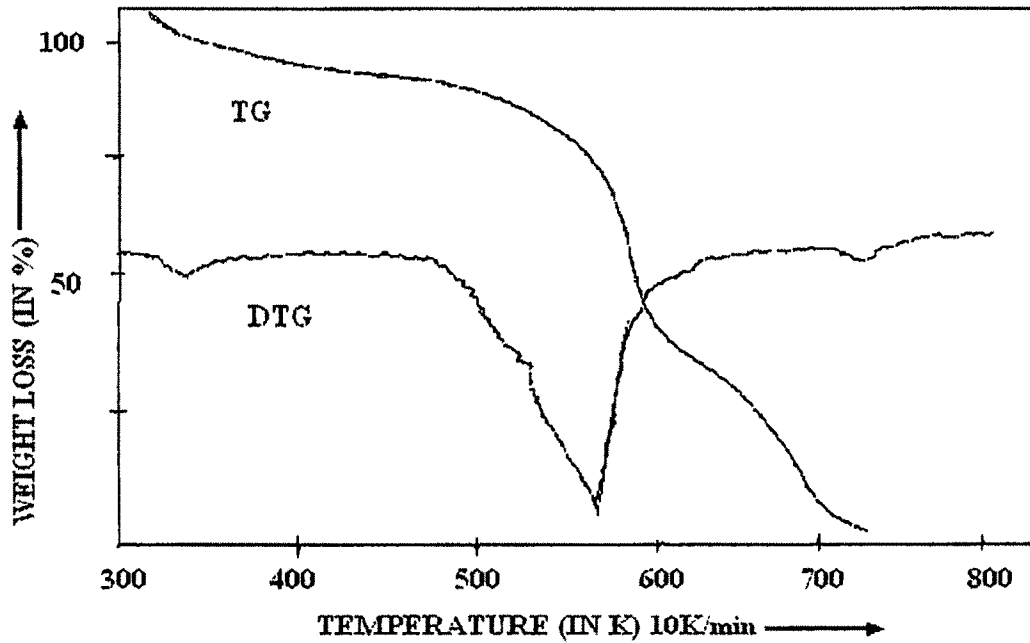


Figure 4.15(b): TG and DTG Thermograms of Sample -B in oxygen atmosphere

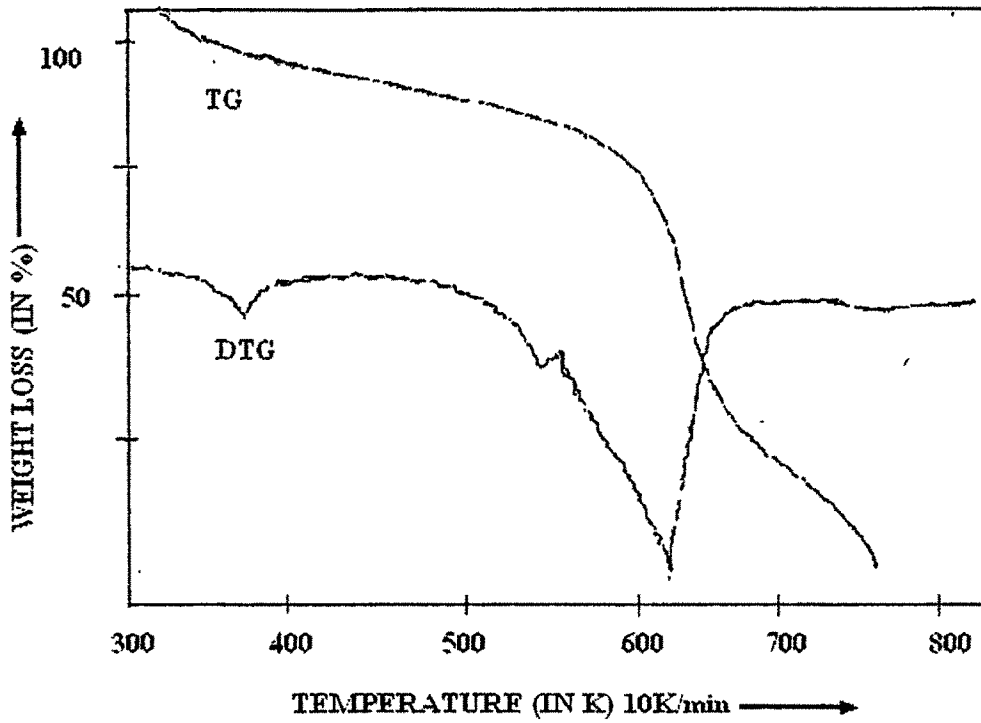


Figure 4.15(c): TG and DTG Thermograms of Sample-B in nitrogen atmosphere

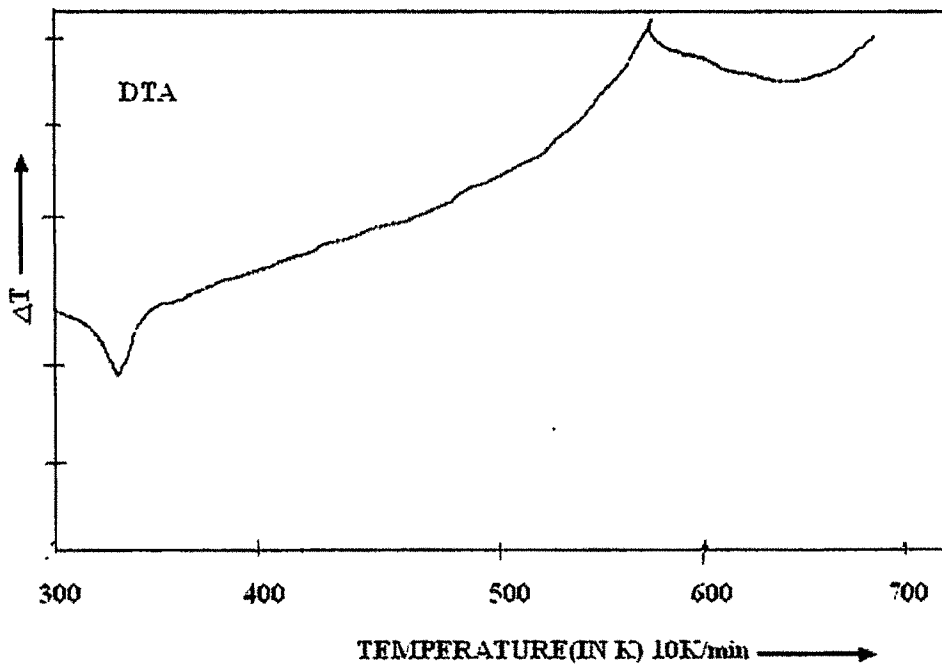


Figure 4.16(a): DTA Thermograms of Sample -B in air atmosphere

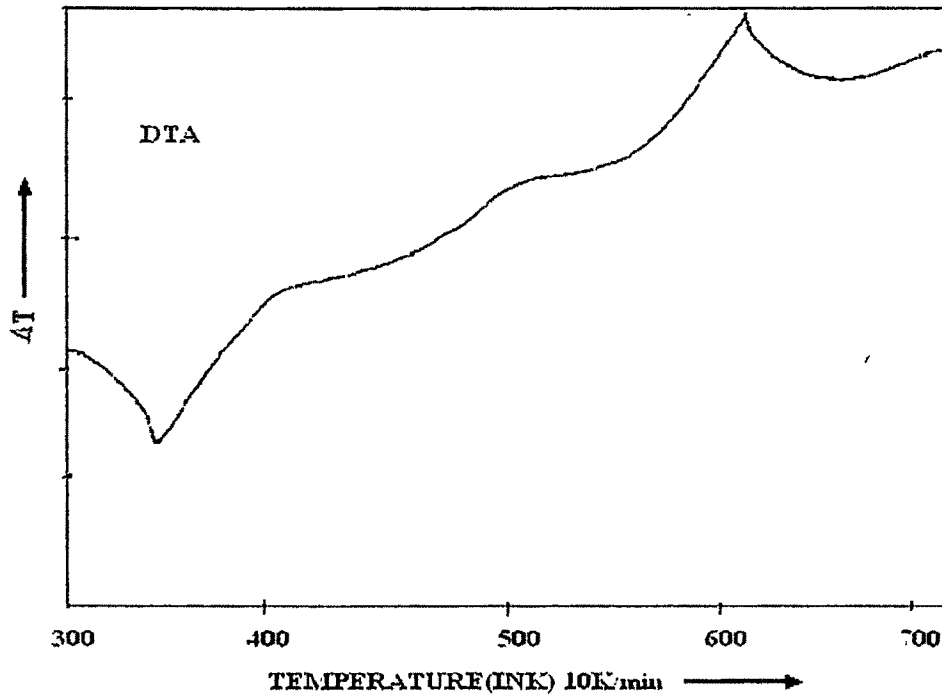


Figure 4.16(b): DTA Thermograms of Sample -B in oxygen atmosphere

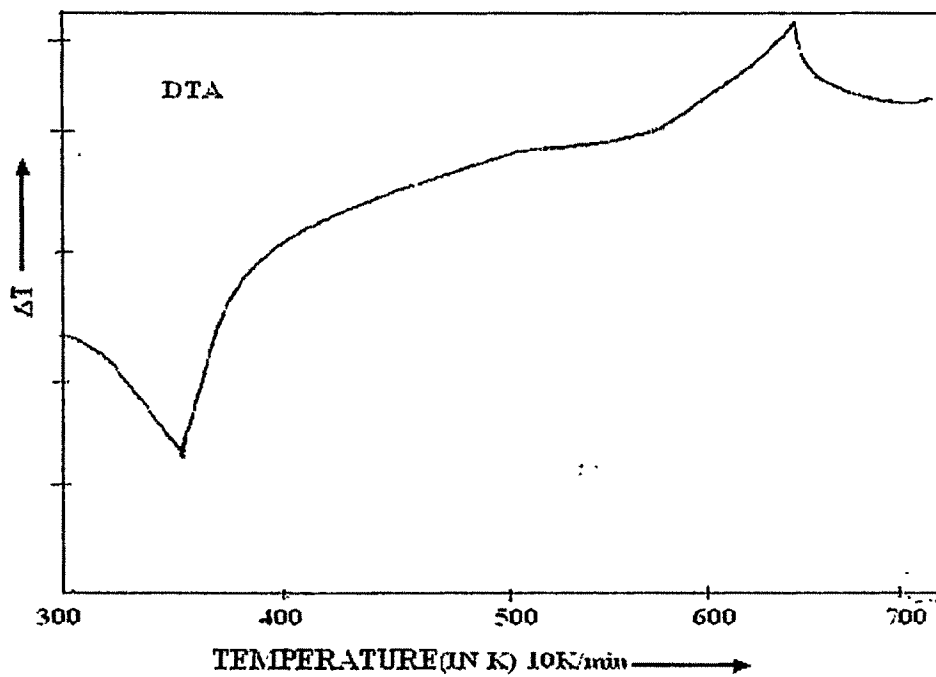


Figure 4.16(c): DTA Thermograms of Sample-B in nitrogen atmosphere

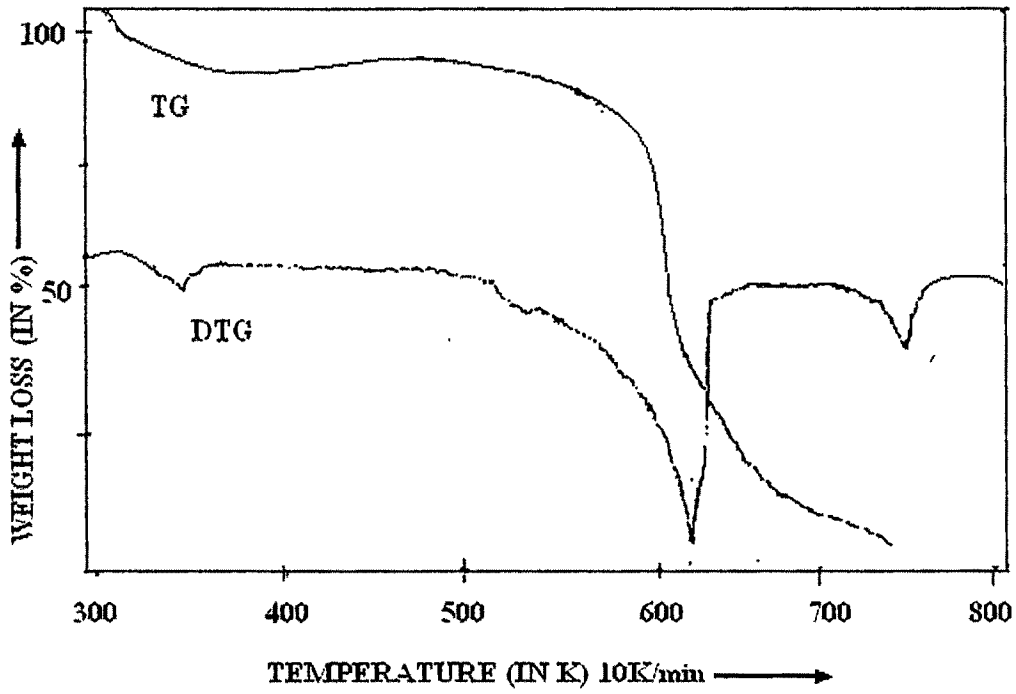


Figure 4.17(a): TG and DTG Thermograms of Sample-C in air atmosphere

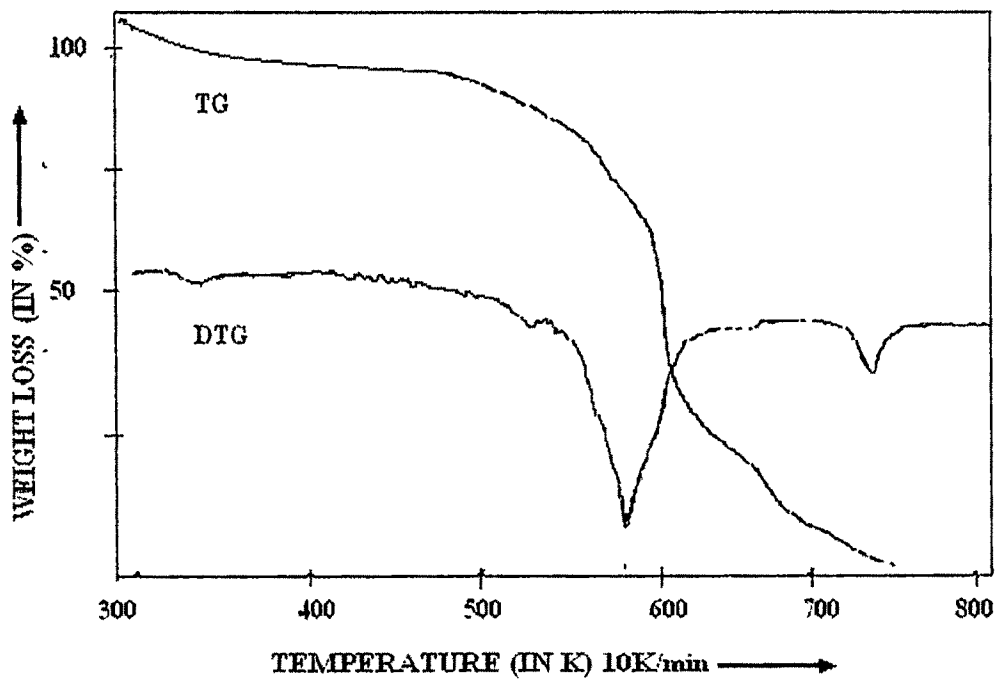


Figure 4.17(b): TG and DTG Thermograms of Sample-C in oxygen atmosphere

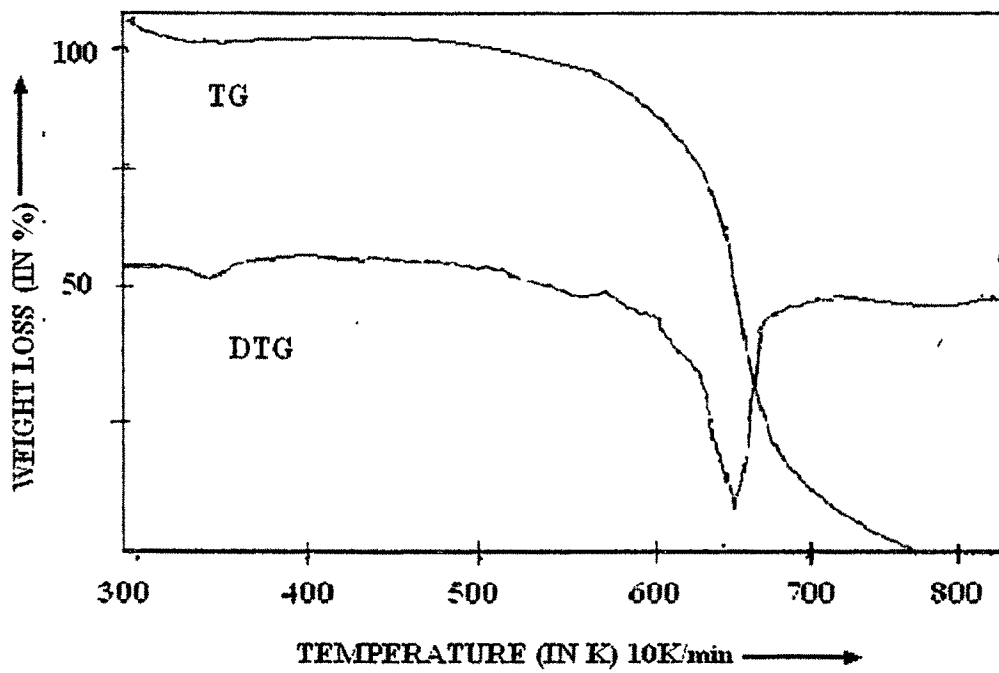


Figure 4.17(c): TG and DTG Thermograms of Sample-C in nitrogen atmosphere

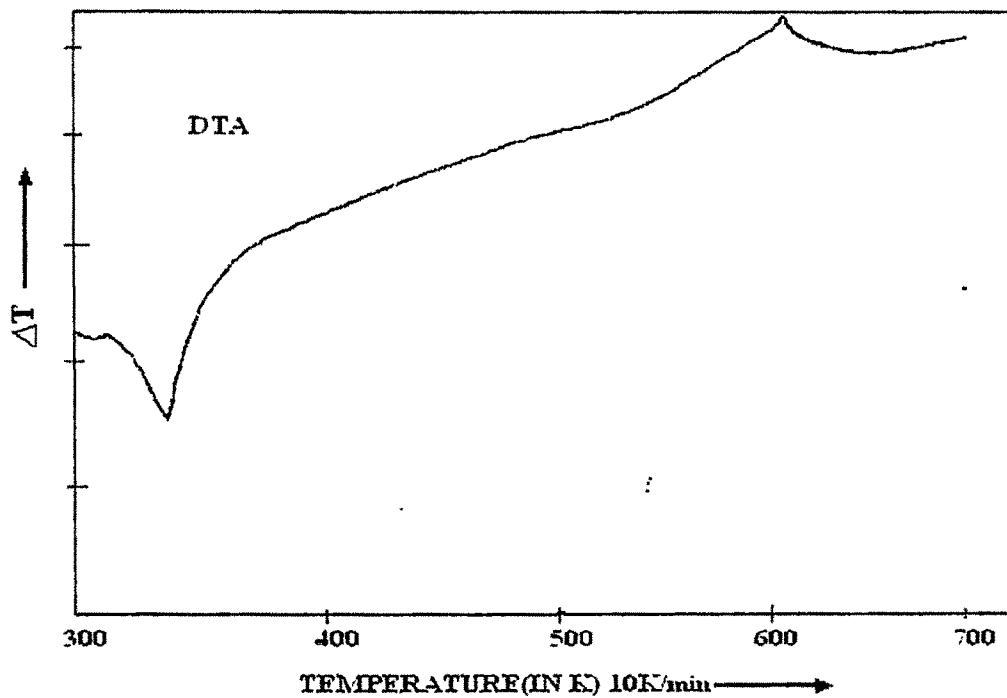


Figure 4.18(a): DTA Thermograms of Sample-C in air atmosphere

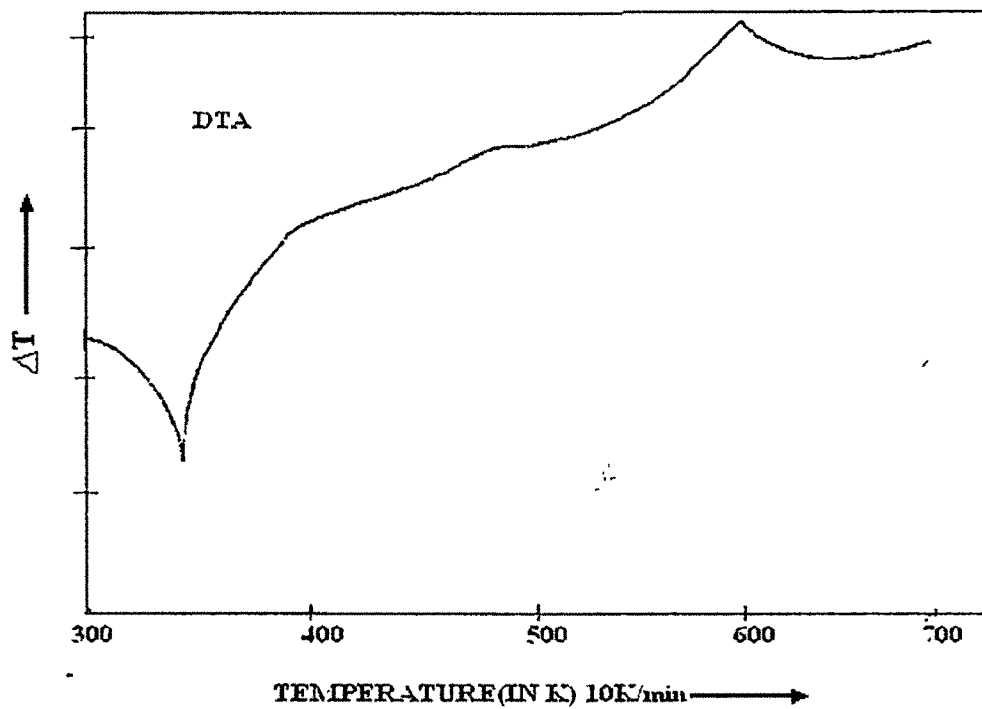


Figure 4.18(b): DTA Thermograms of Sample-C in oxygen atmosphere

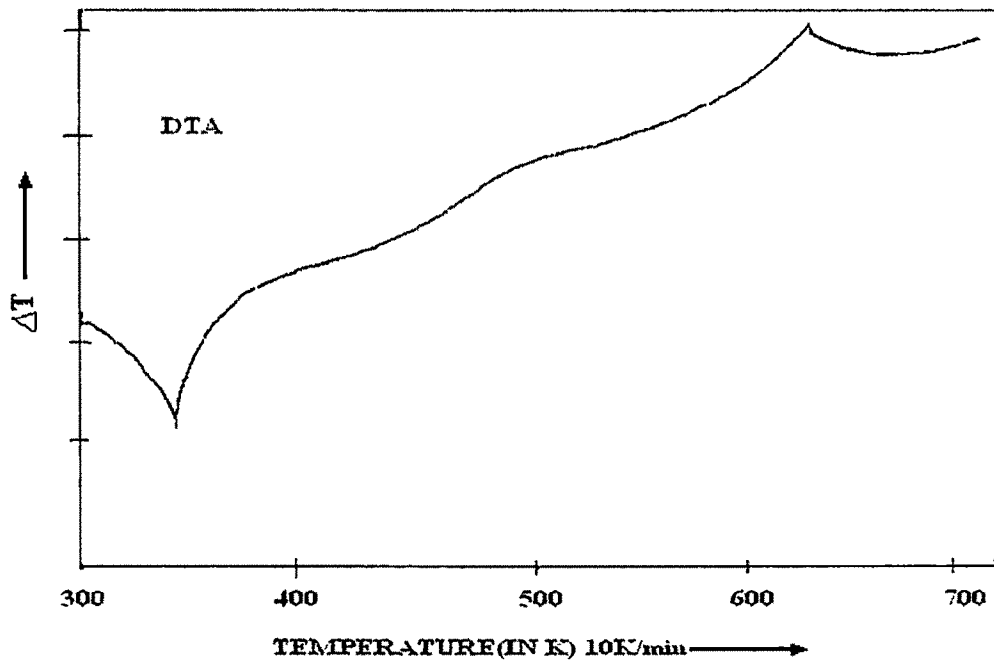


Figure 4.18(c): DTA Thermograms of Sample-C in nitrogen atmosphere

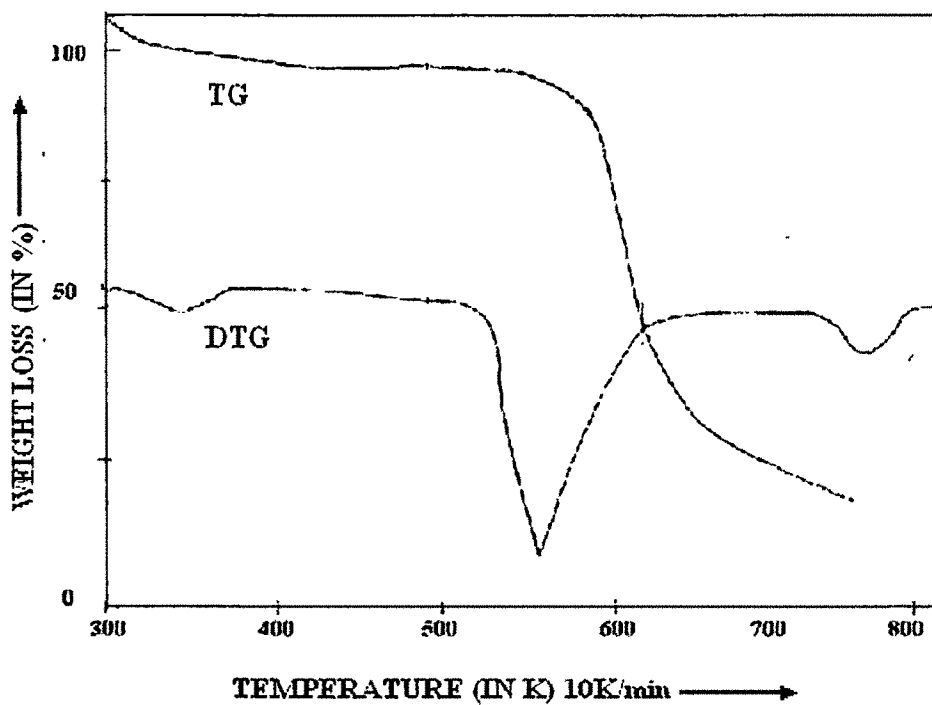


Figure 4.19(a): TG and DTG Thermograms of the sample-D in air atmosphere

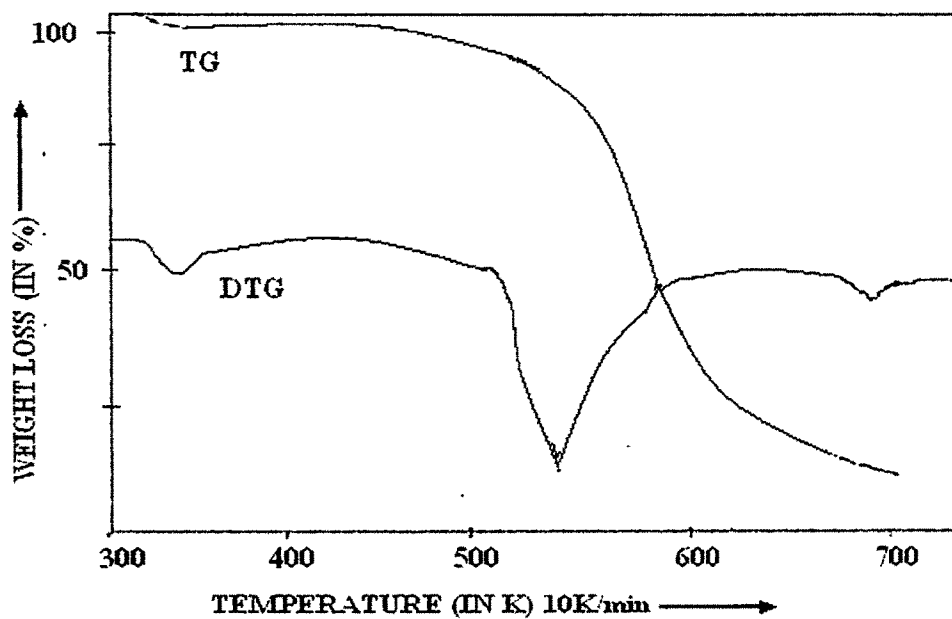


Figure 4.19(b): TG and DTG Thermograms of the sample -D in oxygen atmosphere

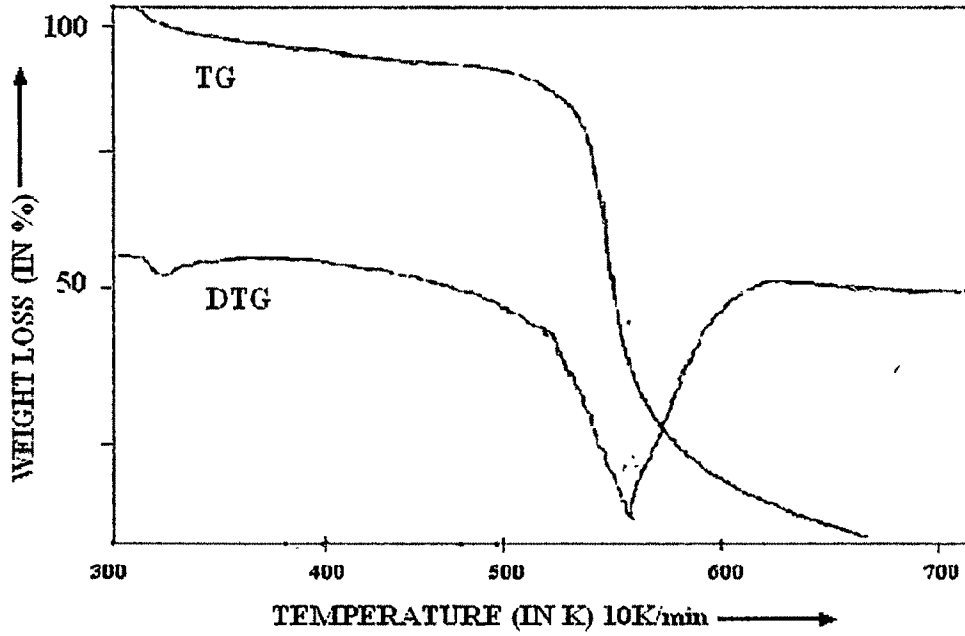


Figure 4.19(c): TG and DTG Thermograms of the sample-D in nitrogen atmosphere

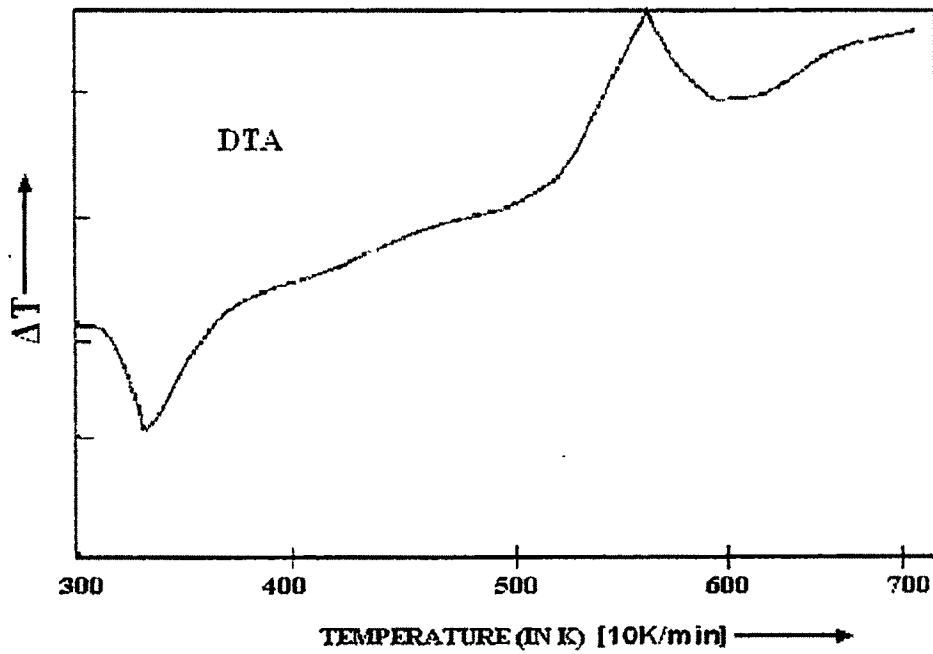


Figure 4.20(a): DTA Thermograms of the sample -D in air atmosphere.

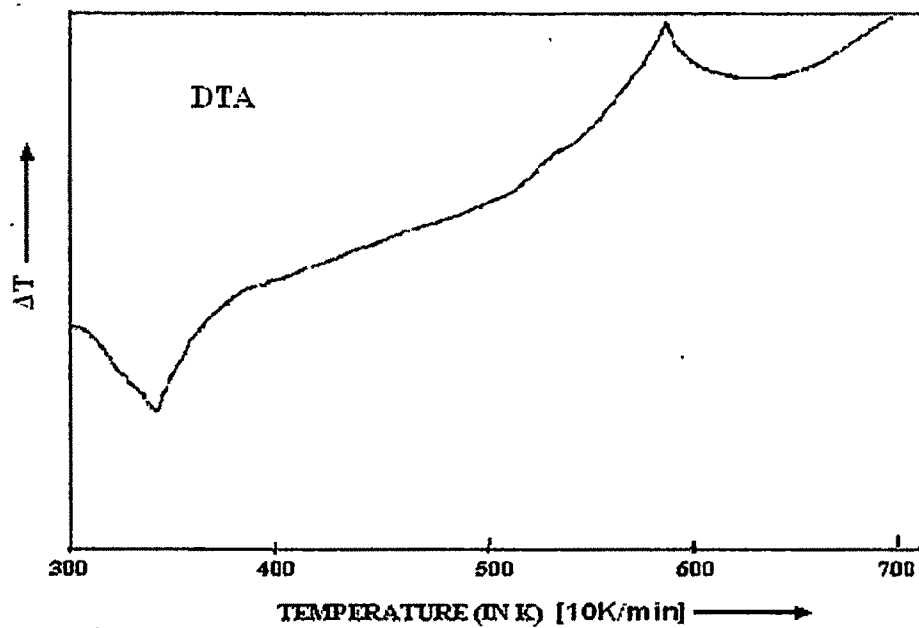


Figure 4.20(b): DTA Thermograms of sample -D in oxygen atmosphere.

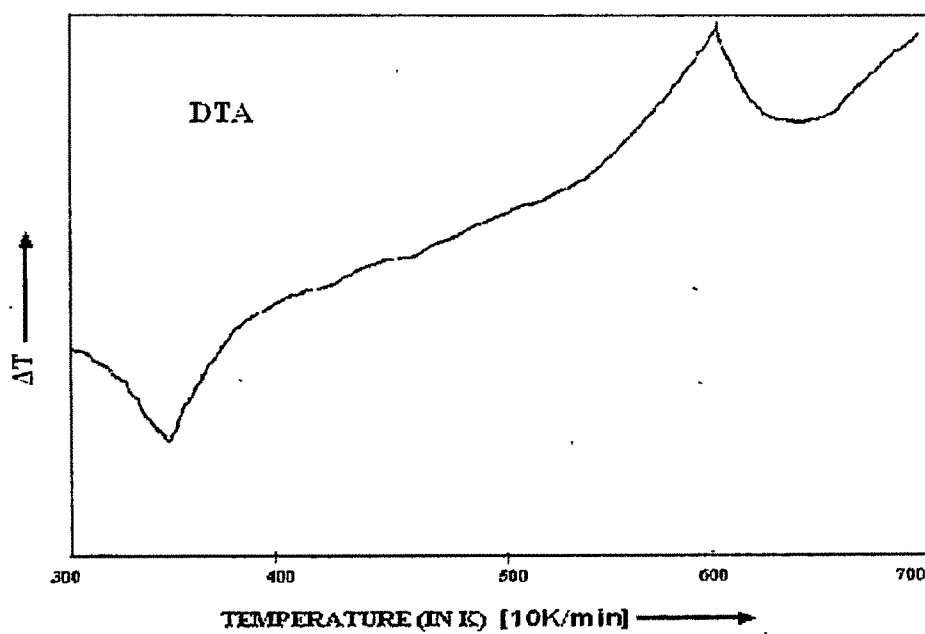


Figure 4.20(c): DTA Thermograms of sample-D in nitrogen atmosphere.

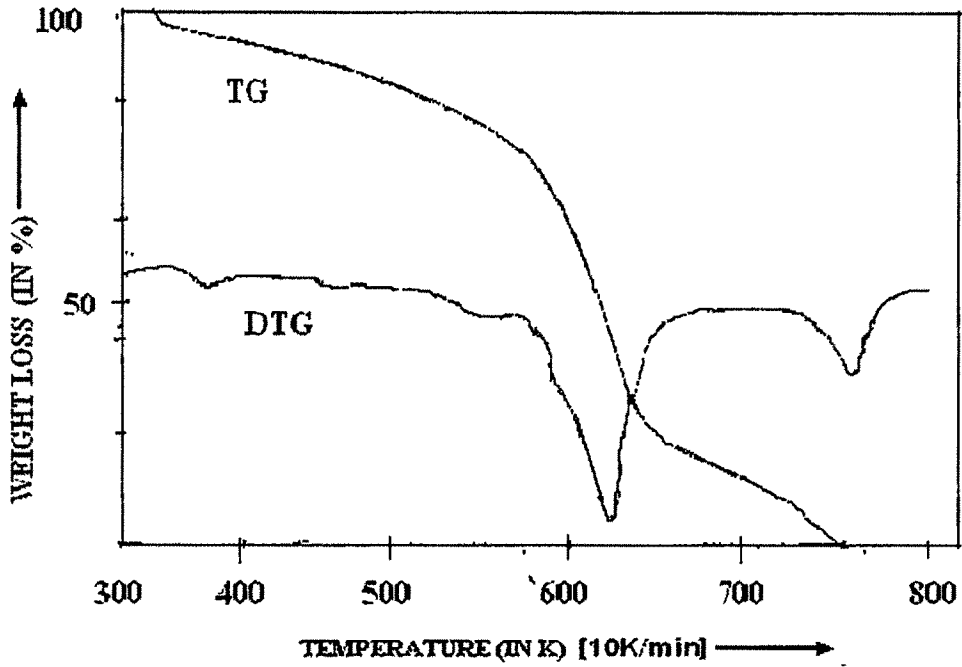


Figure 4.21(a): TG and DTG Thermograms of sample- E in air atmosphere

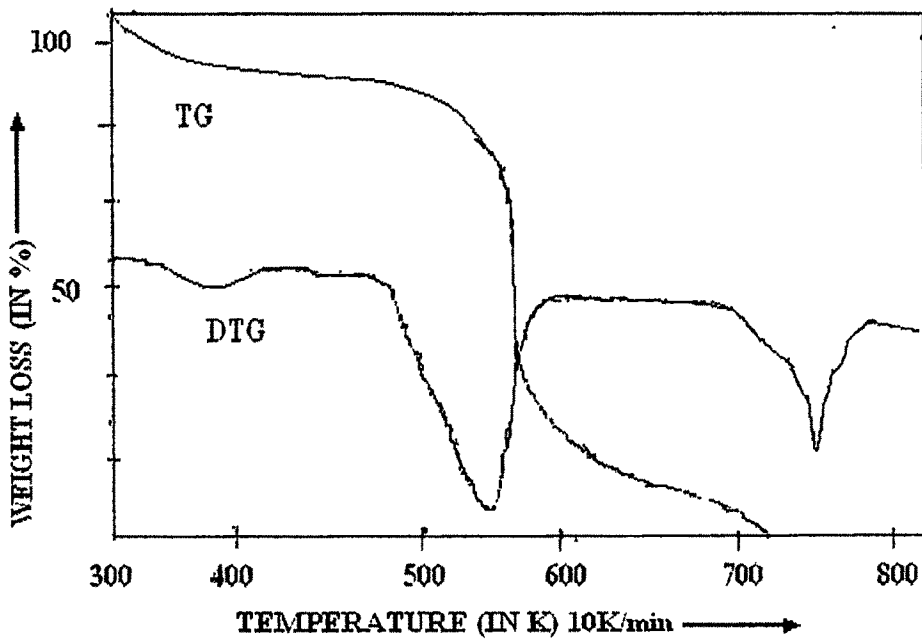


Figure 4.21(b): TG and DTG Thermograms of sample -E in oxygen atmosphere

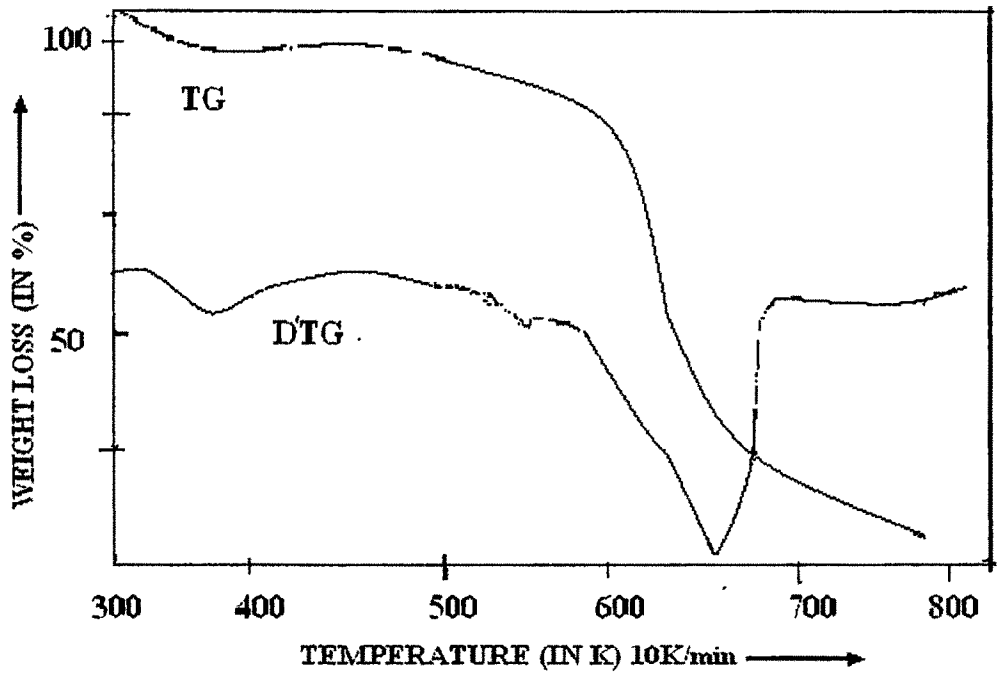


Figure 4.21(c): TG and DTG Thermograms of sample-E in nitrogen atmosphere

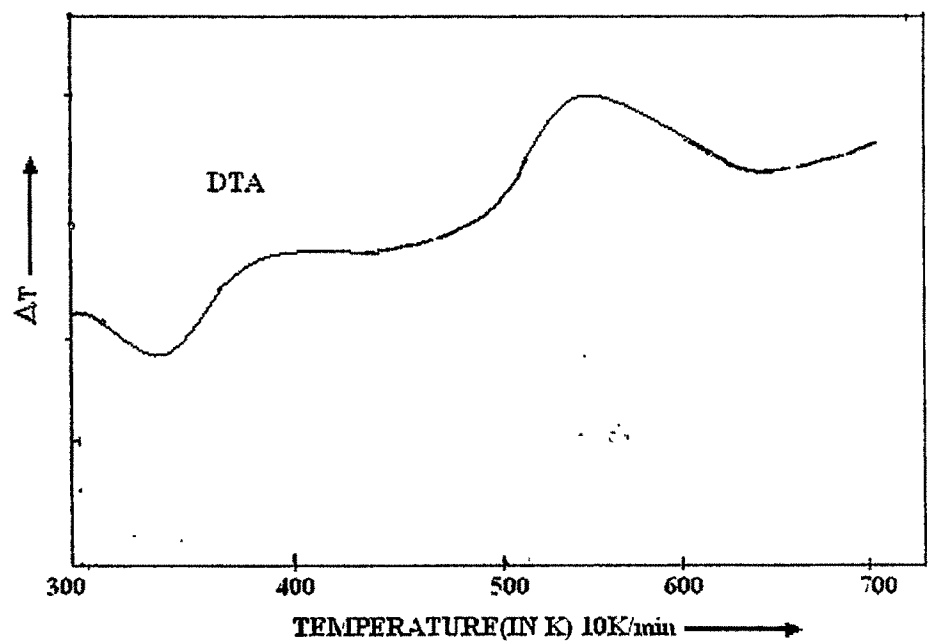


Figure 4.22(a): DTA Thermograms of sample- E in air atmosphere.

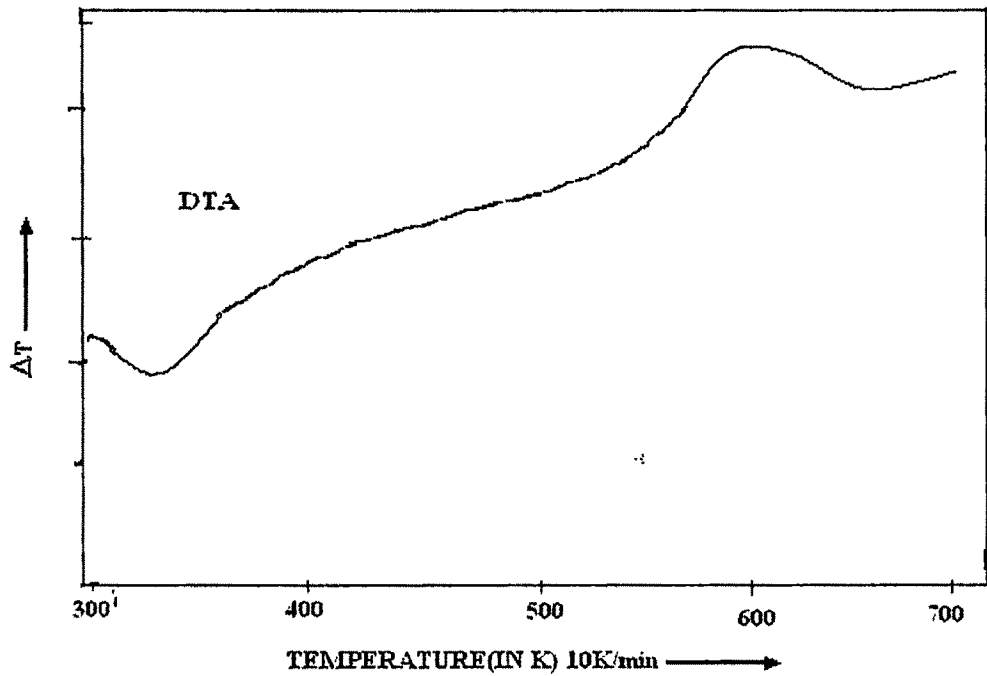


Figure 4.22(b): DTA Thermograms of sample- E in oxygen atmosphere

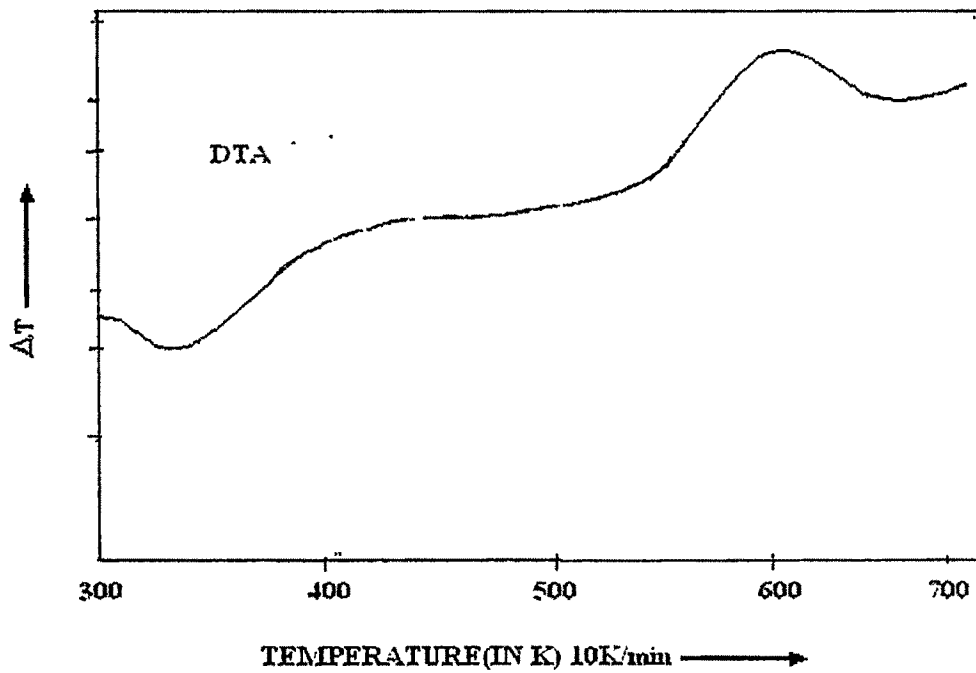


Figure 4.22(c): DTA Thermograms of sample-E in nitrogen atmosphere.

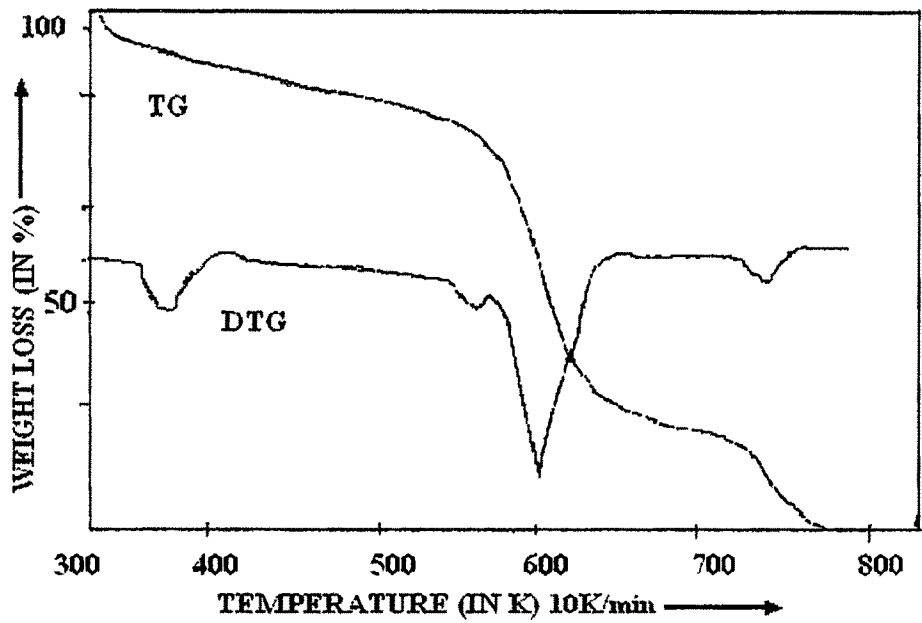


Figure 4.23(a): TG and DTG Thermograms of sample -F in air atmosphere

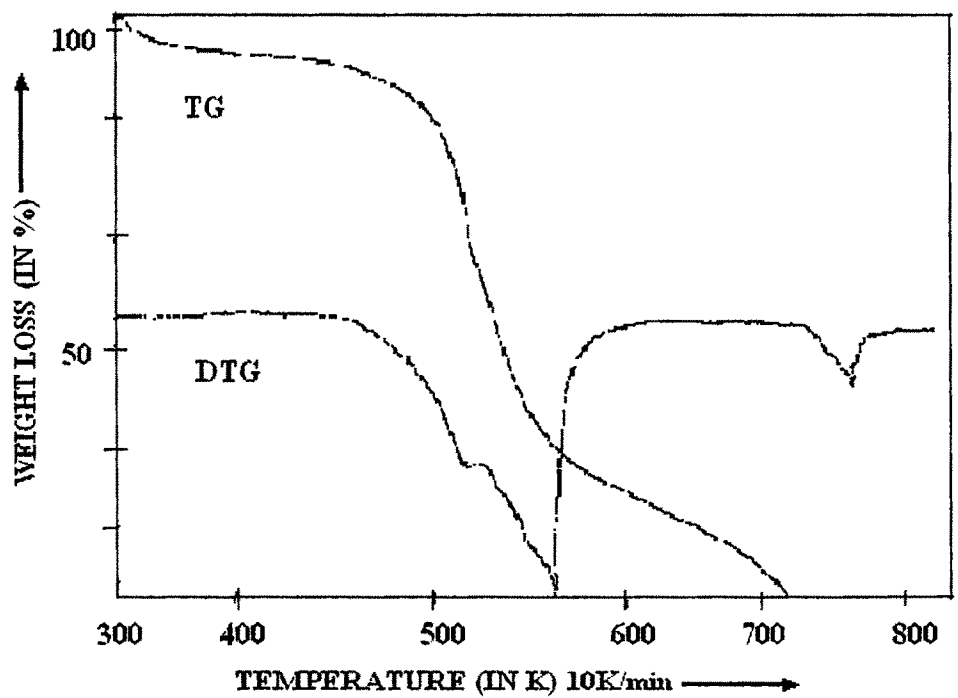


Figure 4.23(b): TG and DTG Thermograms of sample -F in oxygen atmosphere

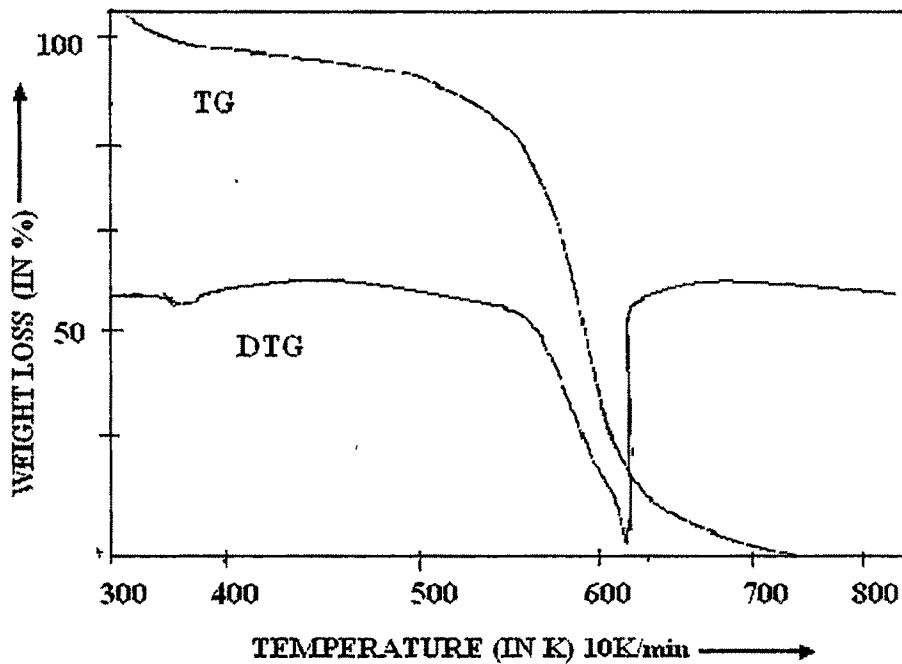


Figure 4.23(c): TG and DTG Thermograms of sample- F in nitrogen atmosphere

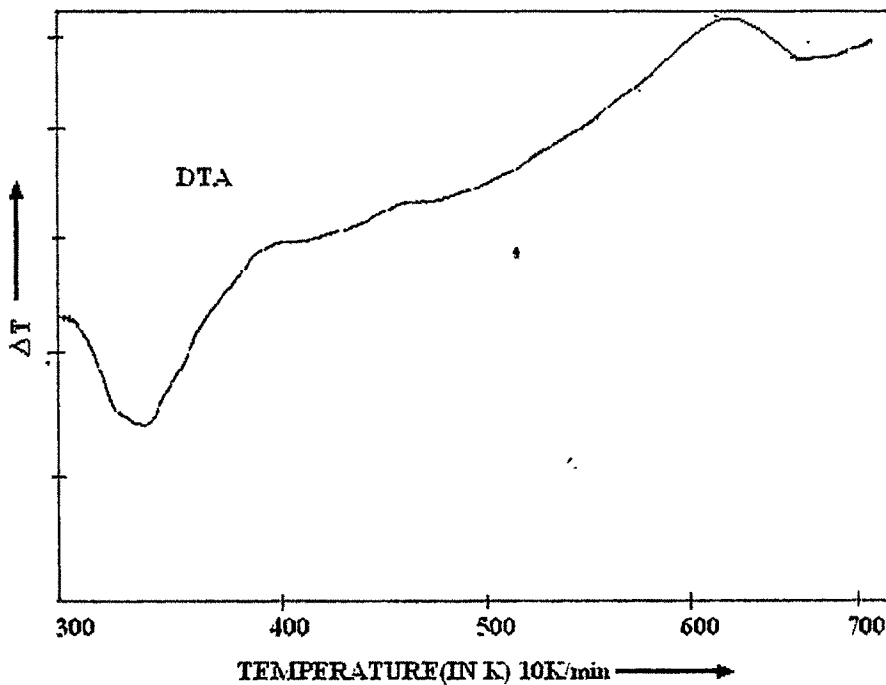


Figure 4.24(a): DTA Thermograms of sample -F in air atmosphere

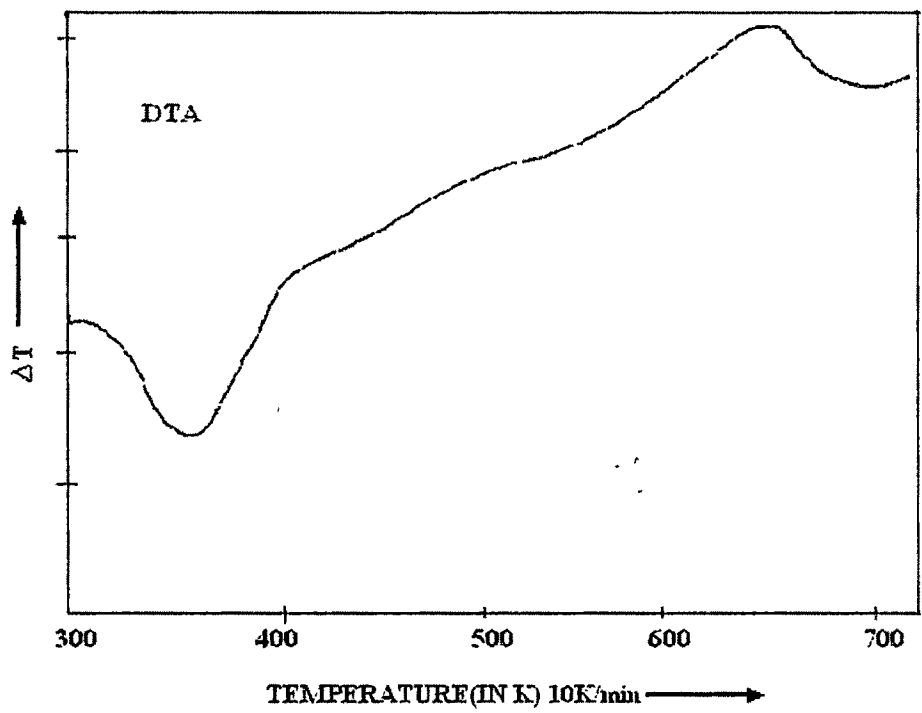


Figure 4.24(b): DTA Thermograms of sample -F in oxygen atmosphere

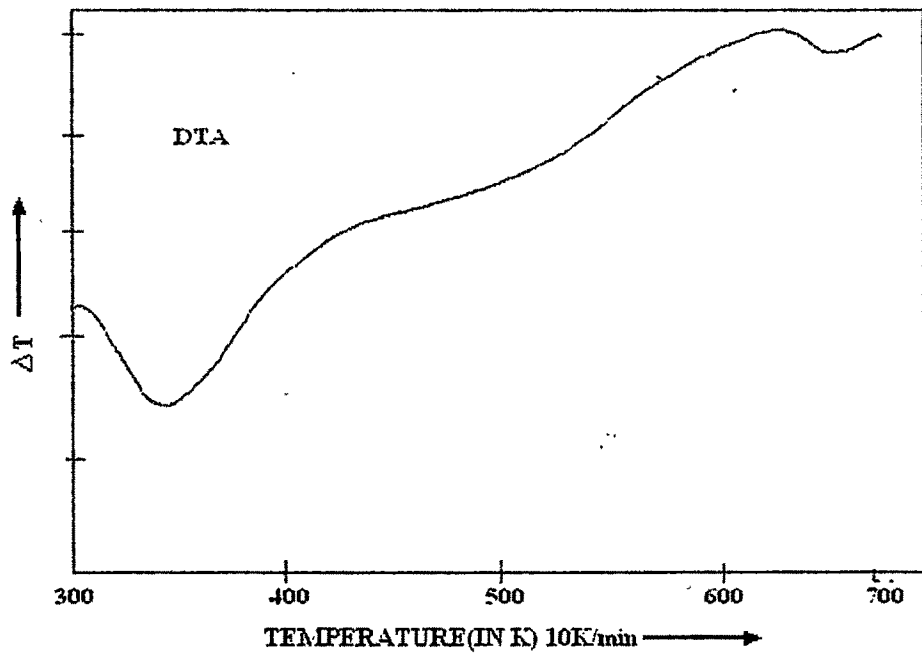


Figure 4.24(c): DTA Thermograms of sample -F in nitrogen atmosphere

4.4 INDEPENDENT DISCUSSION OF THERMAL DECOMPOSITION OF THE SEGMENT

4.4.1 SEGMENT S₁ OF THERMAL DECOMPOSITION FOR THE LEAVES AND FRUITS SAMPLE

In case of leave samples A the TG curve in figure 4.13(a) in air shows that a slow weight loss occurs from 310K and continues up to 375K. This step of TG thermogram is represented by the first endothermic peak in DTG curve. In this temperature range, the weight loss is 4.5%. Corresponding changes are observed in DTG profile of the sample indicating a depression at 329K. The similar weight loss patterns are also observed for the samples in oxygen and nitrogen atmosphere and respective weight loss are found as 4.8% and 6%. DTG in nitrogen shows a depression at about 315K figure 4.13(c), while that no change is observed in oxygen in this temperature range figure 4.22(b). From the first step of TG and DTG thermograms, it is evident that the heat is absorbed by these sample to remove the water molecules embedded in the amorphous region of the semicrystalline plant leaves and fruits. During the process of dehydration the structural process remains unaltered as indicated by the return of the DTG. Thermograms to the base line.

From the figure 4.15, 4.17, 4.19, 4.21 and 4.23, it is observed that the TG of other samples (B, C, D, E & F) also exhibit the similar nature of weight loss as found in case of leaves sample A, in the temperature range approximately 310—375K. The weight loss as of each leaves sample in different atmosphere under consideration, remains almost the same in the temperature range 310—375K and in case of fruits sample the temperature range is 320—385K. In this lower range of temperature, the weight loss for the sample B, C, D, E and F is found to be 6.1, 6.5, 4.2, 5.9 and 5.6 % respectively.

Usually the losses of weakly interacting molecules on heating are reflected in endothermic process in such low temperature range⁷⁻⁸. On the basis of this, endothermic

peak may be assigned to the losses of water molecules from the surface or inter stitches. Since at these temperature range(310—375K) XRD pattern of the sample retained its identity of the XRD pattern of the original sample as discussed in section 4.1;it is convincing that losses of water may not be from the inter stitches of the leaves and fruits. Thus it may be concluded that on thermal treatment at lower range of temperature (310—375K) for leaves sample and (320—385K) for fruits sample, the heat is absorbed by the sample (leaves & fruits) to remove the absorbed water molecules, which are mostly embedded in the amorphous region of the sample. Thus weight loss occurred to all samples during the first step of kinetic reaction may be attributed due to the dehydration process⁹⁻¹⁰

Further all the leave and fruit samples show thermal stability up to approximately 490K. The decomposition processes of the sample are found to be occurred from the temperature above 490K. The TG and DTG results for the samples A, B, C, D, E & F are displayed in tables 4.5, 4.7, 4.9, 4.11, 4.13 & 4.15 respectively.

4.4.2 SEGMENT S₂ OF THERMAL DECOMPOSITION FOR THE SAMPLE

The second segment of TG curve for sample A in air is from 450 to 620K (figure 4.13(a)). In this region the weight loss is 3.9 %. Corresponding DTG of the sample shows the peak at about 559K, which supports the presence of weight loss during the second segments of thermal decomposition. In nitrogen and oxygen atmosphere the TG of the sample A also shows the weight loss. In case of nitrogen (figure 4.13(c)) the weight loss is found to be 35 % in the temperature range 516—654K. In oxygen (figure 4.13(b)) the weight loss is 39.1 % in the 470—590K range.

Similar phenomena are also observed for the leaves and fruits sample B, C, D, E and F. The TG and DTG results of the sample A, B, C, D, E and F are shown in table 4.5, 4.6, 4.7, 4.8, 4.9 and 4.10 respectively.

In the second wide endothermic peaks of DSC (figure 4.25—4.30) in the temperatures 448K, 453K, 423K, 458K, 470K and 465K for the sample A, B, C, D, E and F respectively corresponding to the 2nd segment of TG and DTG results caused by decomposition in the medicinal plant leaves and fruits.

The thermal analysis results of the DSC thermograms is summarized in the Table 4.17. It is evident from the DSC thermograms and reaction kinetic data (Table-4.17) that the dehydration is almost the same for all medicinal plant leaves and fruits. During the dehydration period the initial semi crystalline set up of the plant leaves remains unaltered. This indicates that the absorbed water molecules are mostly embedded in the amorphous region of the leaves.

The second endothermic peak of the samples have attributed to degradation of crystallinity caused by decomposition of molecules. The weight loss is less in the leaves sample and more in fruits sample. From these results of the kinetic data it is assumed that the thermal stability is less in leave samples and more in fruit samples.

The above result reveals that due to heating at these high temperature ranges, i.e. during segment S₂, all the sample decomposed and their crystallinity are totally lost.

Further, in segment S₂, the occurrence of the sharp decrease in weight in TG profile for the sample in air, oxygen and nitrogen atmosphere as shown in figure 4.13,4.15,4.17, 4.19,4.21 and 4.23 indicates the formation of a stable decomposed part of the leave and fruit samples. It is also observed that the decrease in weight for the sample during segment S₂ is found to be more rapid in nitrogen and less in case of oxygen as compared with those in air. This difference of weight loss found in TG profile in

different atmosphere under consideration, during segment S₂, may be attributed due to oxygenation of the leaves and fruits in presence of air and oxygen, where as in nitrogen atmosphere such oxygenation reaction can not be taken place. Thus in case of nitrogen there is more weight loss then in case of oxygen in this region and this also with logic that a hydrocarbon present in sugar will gain weight on oxygenation. In a nutshell these two process can be termed as the thermal decompose (under nitrogen) and thermal oxidative reaction (under oxygen). Similar results were obtained for plant fibre samples by some workers^{6,11}.

4.4.3 SEGMENT S₃ OF THERMAL DECOMPOSITION FOR THE SAMPLE

This segment is occurred only when the TG are performed in oxygen and air. But does not seen in inert atmosphere. The temperature ranges of the segment S₃ and corresponding weight loss occurred of the samples is shown in table 4.5, 4.6, 4.7, 4.8, 4.9 and 4.10.

. A sharp peak is appeared in corresponding DTG profile in oxygen at approximately 690K for sample A (figure 4.13(b)), 720K for sample B (figure 4.15(b)), 750K for sample C (figure 4.17(b)), 700K for sample D (figure 4.19(b)), 738K for sample E (figure 4.21(b)) and 741K for sample F (figure 4.23(b)).

Corresponding changes are well reflected by the exothermic process occurred in DSC in air. An exothermic peak is observed for sample A, B, C, D, E and F in this high temperature range as shown in figure 4.25—4.30. The peak temperature and temperature range of corresponding the exotherms of samples are shown in table 4.17.

Based on these above results the changes observed during this stage of thermal decomposition are attributed due to the formation of carbon dioxide and carbon monoxide gas from the carbonized material that is formed during segment S₃.

Presences of oxygen make it to complete conversion to gaseous material and arial oxidation^{8,10,12}.

The gases thus evolved in the decaying stage are due to thermal degradation. They are traced as water vapour, carbon dioxide and carbon monoxide. In the air and oxygen atmosphere, the weight loss in decaying stage is attributed. This might be due to formation these gases by the process of oxidations where these gases by the process of oxidations where as nitrogen medium, no such oxidations takes place and as a result, the decaying stage were not observed. The decaying stage are shown for the leave and fruit samples A, B, C, D, E and F (air and oxygen atmosphere) in table 4.5, 4.7, 4.9, 4.11, 4.13 and 4.15 respectively.

4.5 DTA RESULTS FOR THE LEAVES & FRUITS SAMPLE

Differential Thermal Analysis (DTA) curves of the leave and fruit samples A, B, C, D, E & F are displayed in figures 4.14, 4.16, 4.18, 4.20, 4.22 and 4.24 in air, oxygen and nitrogen respectively at heating rate 10K/min. The endothermic and exothermic behaviours in DTA thermograms of leaves and fruits at different atmosphere are shown in table 4.5., 4.7, 4.9, 4.11, 4.13 and 4.15 respectively.

In DTA results in table 4.5., 4.7, 4.9, 4.11, 4.13 and 4.15, the endothermic peak temperatures at the lower temperature range for air, oxygen and nitrogen atmosphere are 341K,00K,345K for sample A,330K,342K, 369K for sample B,342K, 334K, 351K, for sample C , 331K, 341K,341K for sample D, 381K,361K,400K for sample E and 347K,336K,370K for sample F respectively. Similarly the exothermic peaks for air, oxygen and nitrogen atmosphere are 555K, 550K, 605K for sample A, 583K, 565K,602K for sample B,610K,590K, 627K for sample C,548K, 560K,562K for sample

D,618K,552K, 662K for sample E and 585K,553K,582K for sample F observed at higher temperature range.

These results indicate that the leave and fruit samples are also hydroscopic in nature.

The exothermic peaks observed in the thermograms of the plant leaves and fruits indicate that decomposition starts (for air, oxygen and nitrogen atmosphere)from 509K,515K,518K for sample A, 410K, 470K, 469K for sample B, 492K,488K,494K for sample C, 503K.516K, 516K for sample D, 492K,490K,495K for sample E and 508K,459K,531K for sample F.

The results of DTA thermograms confirm that all sample show similar dehydration and decomposition reactions under different thermal conditions.DTA results for natural fibres are investigated by some worker³.

4.6 DIFFERENTIAL SCANNING CALORIMETRY (DSC)

The DSC profiling in air of the sample A-Nephafu (*Clerodendron colebrookinum*), B-Mahaneem (*Azadirachta indica*), C-Tulsi (*Ocimum sanctum*), E-Bandordima (*Chisocheton peniculatus*) and F(*Cudrania javenensis*) at the heating rate $10^{\circ}\text{C min}^{-1}$ in air atmosphere are displayed in figure 4.25—4.30 respectively. The peak temperature and temperature range of corresponding endotherms & exotherms of the samples are shown in table 4.17.

The shifting of DSC thermograms from the base line represents the heat capacity of the medicinal plant leave and fruit samples. The DSC traces of the samples show two distinct reactions in two stages after which exothermic reaction is attributed¹³. The first endothermic peak for the samples A, B, C, D, E and F occur at the temperatures 315K,

318K, 308K, 316K, 328K and 325K respectively. But the DSC thermograms of annealed and quenched samples do not attribute such endothermic peaks at these temperatures these phenomena indicate that these endothermic peaks of unheated samples represent the absorption of heat by the samples due to dehydration.

The second wide endothermic peaks in temperatures 448K, 453K, 423K, 458K, 485K and 480K for sample-A, B, C, D, E and F caused by decomposition in the medicinal plant leaves and fruits respectively.

. It is evident from the DSC thermograms and reaction kinetic data (Table-4.17) that the dehydration is almost the same for all these medicinal plant leave and fruit samples. During the dehydration period the initial semi crystalline set up of the plant leave and fruit samples remains unaltered. This indicates that the absorbed water molecules are mostly embedded in the amorphous region of the leave and fruits samples.

The second endothermic peak of the samples have attributed to degradation of crystallinity caused by decomposition of molecules. The weight loss is less in the leave sample C and more in sample B than that in the samples A & D. From these results of the kinetic data it is assumed that the thermal stability is less in the sample C and more in B than in A & D. Again the weight loss is more for the fruit sample E than that in fruit sample F. These results of the kinetic data indicate that the thermal stability is less in the fruit sample F than that of fruit sample E. and also it is assumed that the weight losses are less in leave samples than that in fruit samples. It is establish that the thermal stability is more in the fruit samples than that of the leave samples.

4.7 EVALUATION OF KINETIC DATA

The activation energy(E_1) required to activate the thermal reactions in dehydration and decomposition stages, on heating for sample A, B, C, D, E and F in air,

oxygen and nitrogen atmospheres are evaluated by Freeman and Coarroll differential method from their respective TG slopes as used earlier¹⁴ to evaluate (E_1) for some polymers.

The activation energy (E_1) values computed from TG and DTG curves are slightly higher in oxygen atmosphere and smaller in nitrogen atmosphere than in air atmosphere. Activations Energy (E_1) computed from TG and DTG thermograms for the sample A, B, C, D, E and F under different media (Air, Oxygen & Nitrogen) are shown in tables 4.6, 4.8, 4.10, 4.12, 4.14 and 4.16 respectively. Again the peak temperature, weight loss and activation energy of DSC thermograms are included in table 4.17. From the values of activation energy it is evident that in case of all leaves and fruits the energy required to activate dehydration is less than that required to activate the decomposition reactions. The activation energy involved in both dehydration and decomposition reactions is higher in the leave samples B & C and smaller in the sample A than that of sample D.

Similarly in case of fruits the activation energy involved in both dehydration and decomposition reactions are higher in the sample E and smaller in the sample F. The DSC profile in air showed both endothermic and exothermic peaks for all samples.

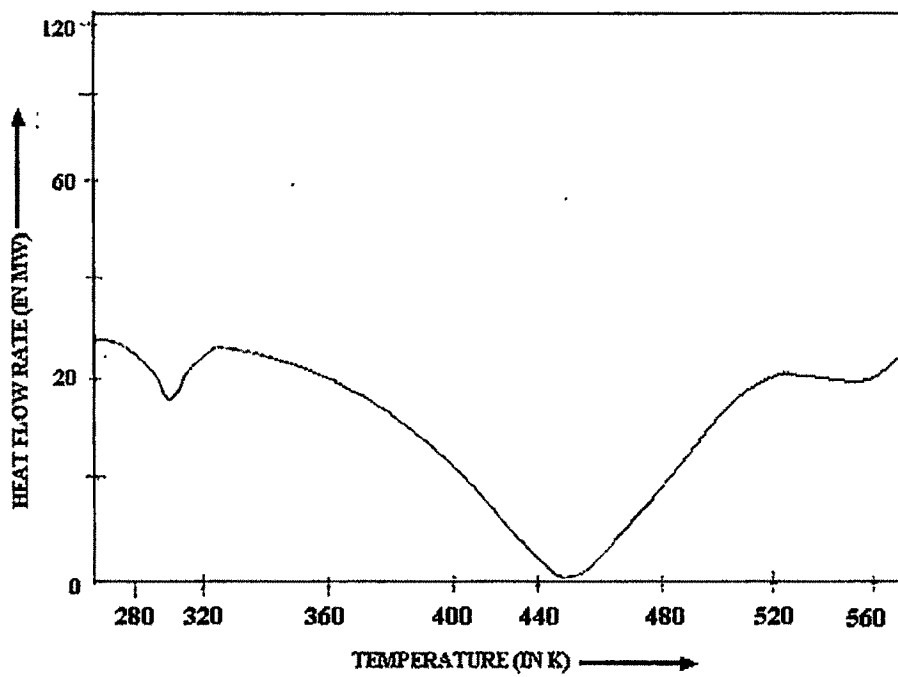


Figure 4.25: DSC Thermograms of medicinal plant leaves sample A

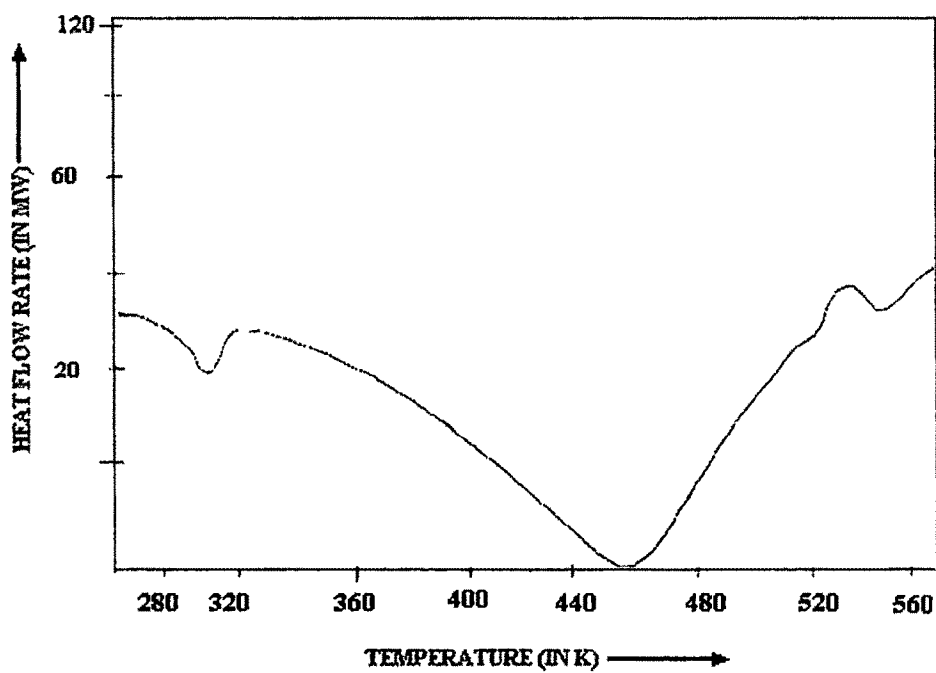


Figure 4.26: DSC Thermograms of medicinal plant leaves sample B

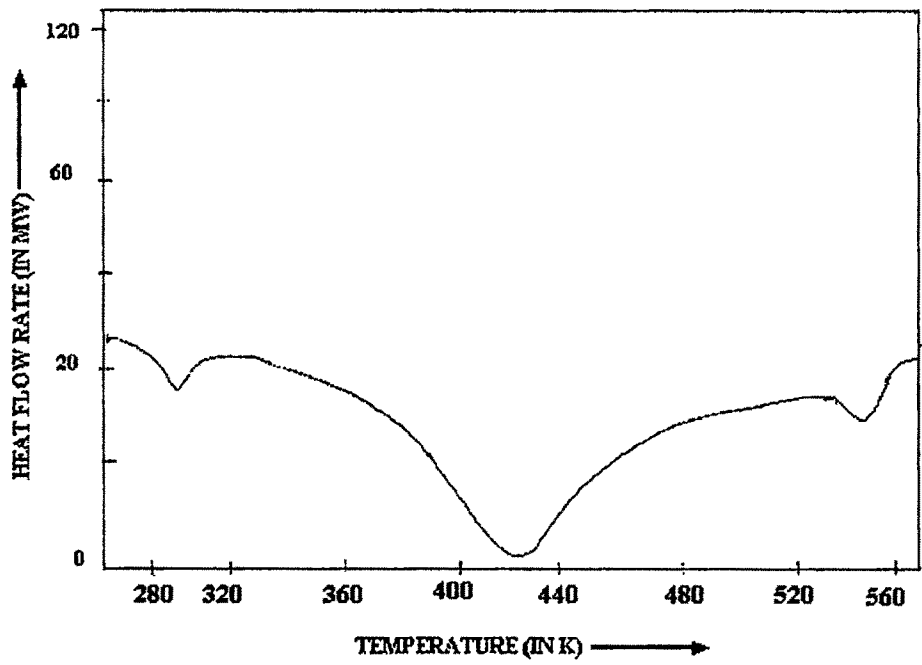


Figure 4.27: DSC Thermograms of medicinal plant leaves sample C

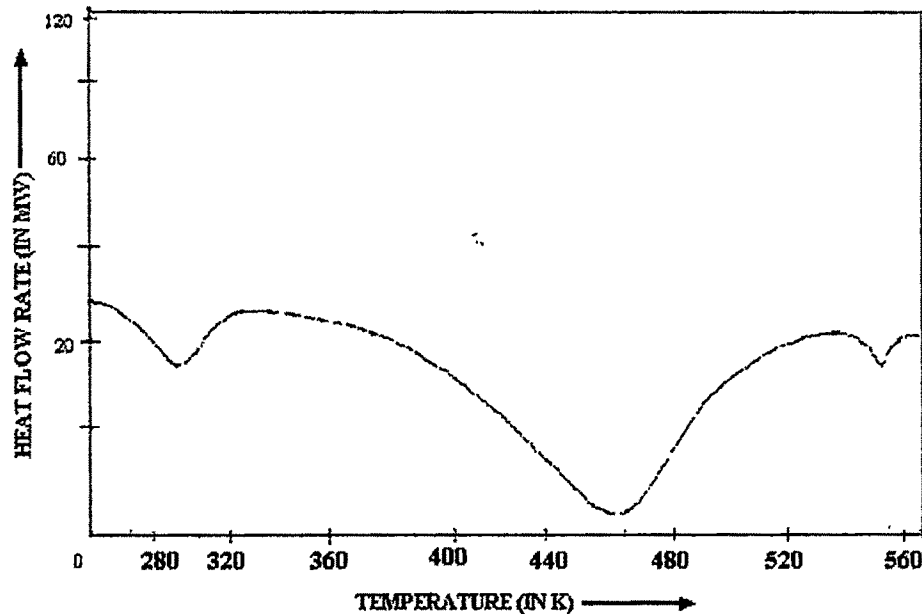


Figure 4.28: DSC Thermograms of medicinal plant leaves sample D

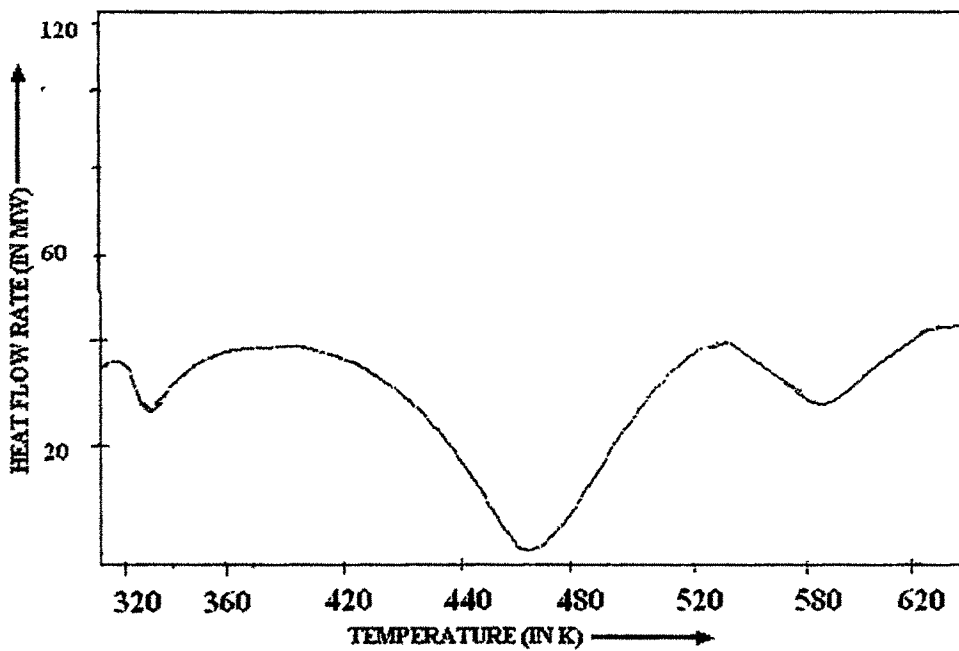


Figure 4.29: DSC Thermograms of medicinal plant fruits sample E

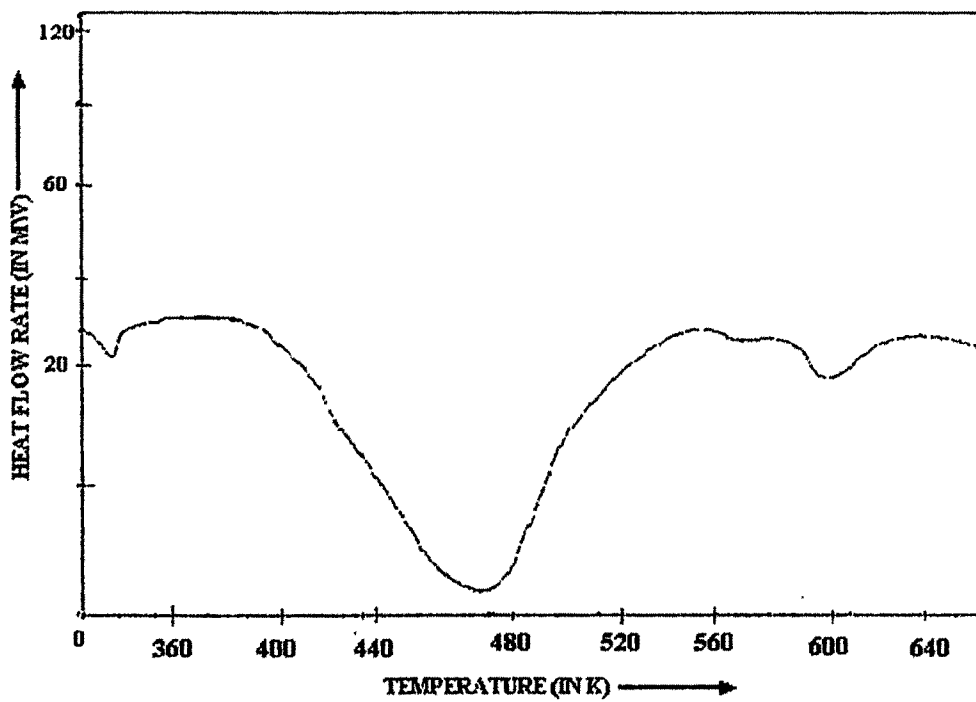


Figure 4.30: DSC Thermograms of medicinal plant fruits sample F

Table 4.5. TG, DTG and DTA Data under different media (Air, Oxygen and Nitrogen) for sample A

Sample	Medium	Step	TG Data		DTG Data		DTA Data		Remarks
			Temp. range	Weight Loss%	Temp. range	Peak Temp	Temp. range	Peak. Temp	
A	air	1	310-375	4.5	312-360	335	313-353	341	Dehydration
		2	450-620	3.9	480-605	559	509-615	555	Decomposition
		3	678-723	10.9	690-730	690	635-690	683	Decaying
	oxygen	1	312-350	5.7	-----	---	-----	---	-----
		2	470-590	39.1	515-559	530	515-610	550	Decomposition
		3	690-715	12.0	685-711	695	685-700	690	Decaying
	nitrogen	1	317-359	4.8	318-365	350	320-360	345	Dehydration
		2	516-654	35	513-562	580	518-615	605	Decomposition

Table 4.6: Activations Energy (E) and change of entropy (ΔS) computed from TG & DTG thermograms of sample (A) under different media (Air, Oxygen & Nitrogen) for sample A

Step	Air Atmosphere		Oxygen atmosphere		Nitrogen Atmosphere	
	E	ΔS	E	ΔS	E	ΔS
	(KJmol ⁻¹)	(e.u)	(KJmol ⁻¹)	(e.u)	(KJmol ⁻¹)	(e.u)
1	11.80	-135.41	17.31	-152.21	12.50	-158.31
2	46.70	-175.01	67.20	-164.41	54.11	-173.90

Table 4.7: TG, DTG and DTA Data under different media (Air, Oxygen and Nitrogen) for sample B

Sample	Medium	Step	TG Data		DTG Data		DTA Data		Remarks
			Temp. range	Weight Loss%	Temp. range	Peak Temp	Temp. range	Peak. Temp	
B	air	1	308-350	6.1	375-355	340	307-350	330	Dehydration
		2	460-605	40	470-602	580	410-592	583	Decomposition
		3	735-775	13	735-760	750	520-750	742	Decaying
	oxygen	1	307-340	7.8	309-345	340	306-346	342	Dehydration
		2	465-613	41	467-615	560	470-620	565	Decomposition
		3	670-735	12.1	662-730	730	665-725	720	Decaying
	nitrogen	1	315-369	7.5	317-372	352	312-376	369	Dehydration
		2	460-610	39	461-625	610	469-628	602	Decomposition

Table 4.8: Activations Energy (E_1) and change of entropy (ΔS) computed from TG & DTG thermograms of sample B under different media (Air, Oxygen & Nitrogen)

Step	Air Atmosphere		Oxygen atmosphere		Nitrogen Atmosphere	
	E	ΔS	E	ΔS	E	ΔS
	(KJmol ⁻¹)	(e.u)	(KJmol ⁻¹)	(e.u)	(KJmol ⁻¹)	(e.u)
1	15.52	-147.61	17.75	-156.52	16.12	-143.34
2	47.35	-179.72	65.32	-180.11	55.10	-172.56

Table 4.9: TG, DTG and DTA Data under different media (Air, Oxygen and Nitrogen) for sample C

Sample	Medium	Step	TG Data		DTG Data		DTA Data		Remarks
			Temp. range	Weight Loss%	Temp. range	Peak Temp	Temp. range	Peak Temp	
C	air	1	309-365	6.5	311-670	345	310-372	342	Dehydration
		2	485-630	37.2	490-635	615	492-632	610	Dehydration
		3	710-772	12.3	715-780	760	705-778	755	Decaying
	oxygen	1	312-370	6.9	315-376	339	312-372	334	Dehydration
		2	487-615	39.6	490-620	595	488-615	590	Decomposition

		3	713-782	13.1	715-788	752	713.6	750	Decaying
	nitrogen	1	317-372	6.7	319-379	355	316-375	351	Dehydration
		2	495-689	38.7	492-685	630	494-688	627	Decomposition

Table 4.10. Activations Energy (E_1) and change of entropy (ΔS) computed from TG & DTG thermograms of sample C under different media (Air, Oxygen & Nitrogen)

Step	Air Atmosphere		Oxygen atmosphere		Nitrogen Atmosphere	
	E_1 (KJmol ⁻¹)	ΔS (e.u)	E_1 (KJmol ⁻¹)	ΔS (e.u)	E_1 (KJmol ⁻¹)	ΔS (e.u)
1	14.45	-156.31	16.56	-162.28	15.80	-149.32
2	48.12	-169.31	63.10	-178.54	53.31	-162.96

Table 4.11. TG, DTG and DTA Data under different media (Air, Oxygen and Nitrogen)
for sample D

Sample	Medium	Step	TG Data		DTG Data		DTA Data		Reactions
			Temp. range	Wight loss %	Temp range(k)	Peak Temp.	Temp. Range	Peak Temp.	
D	Air	1	306-370	4.2	308-362	340	310-350	331	Dehydration
		2	515-618	41.0	510-615	551	503-609	548	Dehydration
		3	680-719	12.0	681-720	692	682-721	699	Decaying
	Oxygen	1	308-367	6.8	310-368	348	309-371	341	Dehydration
		2	518-612	42.0	516-611	553	516-612	560	Decomposition
		3	699-720	15.1	698-719	702	692-707	700	Decaying
	Nitrogen	1	310-368	4.6	313-367	346	313-368	341	Dehydration
		2	511-611	38.1	513-612	555	516-613	562	Decomposition

Table 4.12. Activations Energy (E) and change of entropy (ΔS) computed from TG & DTG thermograms of sample D under different media (Air, Oxygen & Nitrogen)

Step	Air Atmosphere		Oxygen atmosphere		Nitrogen Atmosphere	
	E_1 (KJmol ⁻¹)	ΔS (e.u)	E_1 (KJmol ⁻¹)	ΔS (e.u)	E_1 (KJmol ⁻¹)	ΔS (e.u)
1	12.80	-140.41	14.61	-142.31	11.50	-138.21
2	38.70	-170.01	52.20	-172.41	50.21	-168.78

Table 4.13: TG, DTG and DTA Data under different media (Air, Oxygen and Nitrogen)

for sample E

Sample	Medium	Step	TG Data		DTG Data		DTA Data		Remarks
			Temp. range	Weight Loss %	Temp. range	Peak temp.	Temp. range	Peak temp.	
E	air	1	320-385	5.9	325-382	365	322-383	361	Dehydration
		2	492-689	9.2	490-688	620	492-690	618	Decomposition
		3	705-791	13.3	703-789	760	701-790	756	Decaying
	oxygen	1	325-435	11.2	327-436	365	323-431	361	Dehydration
		2	490-594	49.3	492-592	550	490-590	552	Decomposition
		3	679-750	20.6	682-754	735	680-756	738	Decaying
	nitrogen	1	326-405	15.5	327-402	390	325-404	400	Dehydration
		2	497-685	46.6	495-682	667	495-687	662	Decomposition

Table 4.14: Activations Energy (E_1) and change of entropy (ΔS) computed from TG &

DTG thermograms of sample E under different media (Air, Oxygen & Nitrogen)

Step	Air Atmosphere		Oxygen atmosphere		Nitrogen Atmosphere	
	E_1 (KJmol ⁻¹)	ΔS (e.u)	E_1 (KJmol ⁻¹)	ΔS (e.u)	E_1 (KJmol ⁻¹)	ΔS (e.u)
1	19.71	-160.46	21.52	-166.22	21.47	-158.72
2	58.11	-190.26	72.22	-192.61	69.20	-179.66

Table 4.15. TG, DTG and DTA Data under different media (Air, Oxygen and Nitrogen)

for sample F

Sample	Medium	Step	TG Data		DTG Data		DTA Data		Remarks
			Temp. range	Weight Loss %	Temp. range	Peak Temp	Temp. range	Peak Temp	
F	air	1	321-380	5.6	324-385	345	326-383	347	Dehydration
		2	505-615	15.2	610-611	590	508-614	585	Decomposition
		3	715-785	22.1	713-787	760	710-782	756	Decaying
	oxygen	1	308-379	14.1	305-376	332	310-372	336	Dehydration
		2	462-615	48.2	460-620	557	459-622	553	Decomposition
		3	703-770	27.6	705-772	742	338-401	741	Decaying
	nitrogen	1	345-402	29.1	341-406	372	338-401	370	Dehydration
		2	535-630	45.4	532-632	585	531-625	582	Decomposition

Table 4.16: Activations Energy (E_1) and change of entropy (ΔS) computed from TG & DTG thermograms of sample F under different media (Air, Oxygen & Nitrogen)

Step	Air Atmosphere		Oxygen atmosphere		Nitrogen Atmosphere	
	E_1	ΔS	E_1	ΔS	E_1	ΔS
	(KJmol^{-1})	(e.u)	(KJmol^{-1})	(e.u)	(KJmol^{-1})	(e.u)
1	17.56	-160.51	16.84	-169.44	18.51	-158.26
2	50.62	-190.79	67.41	-192.45	60.31	-191.52

Table 4.17: Reaction kinetic data of the DSC thermograms at transition periods.

Sample	Heating Rate K/min	Step	Peaks Temp.in (K)	Weight Loss (%)	Activa Energy KJ/mol	Reaction
A	10	1	315	21	8.23	Dehydration
		2	448	68	21.38	Decomposition
B	10	1	318	22	10.34	Dehydration
		2	453	76	28.20	Decomposition
C	10	1	308	16	5.82	Dehydration
		2	423	52	18.38	Decomposition
D	10	1	316	21.2	8.31	Dehydration
		2	458	78	25.1	Decomposition
E	10	1	328	27.2	12.4	Dehydration
		2	489	120	34.6	Decomposition
F	10	1	325	27.5	16.7	Dehydration
		2	485	78.7	31.3	Decomposition

CONCLUSION

From the investigations with different physical methods, it has been confirmed that the medicinal plant leave and fruit samples have absorption and desorption behaviours. Thermal stability is more for the fruit samples than the leave samples All the medicinal plant leave and fruit samples are semicrystalline and hydrophilic in nature. The first, second and third transition points of thermograms of leave and fruit samples represent dehydration, decomposition and degradation of Crystalline setup. No significant variation of thermal activities of the samples in different atmospheres (Air, Oxygen & Nitrogen) has attributed.

REFERENCES: 4

1. Bartram S.F, Hand Book of X-rays, McGraw-Hill Book Co.Ltd., Landon, 1967, Chapter 17-21.
2. Baruah G.C., Ph.D.Thesis entitled "Studies on the thermop-hysical properties of some organic complex(fibres) by X-ray diffraction and other physical method ", Gauhati University., (1991)
3. Taluckdar C.L., Ph.D.Thesis entitled "An investigation on thermop-hysical behaviours of some fibre readily available in the north eastern region of India by various physical method ", Gauhati University., (1991)
4. Baruah G.C., M.N.Bora, *J.Assam Sci.Soc*, 31(1), 1988, 66
5. Bardoloi.S, Ph.D.Thesis entitled "Crystallographic study of some polymer (plant and silk fibres) and similar monomer (Glycocyamine Complex)", Gauhati University, 1998
6. Jaffe.M., in Thermal Characterization of polymeric materials, E.A.Turi, Eds. Academic press Ins., London, 1981, 709pp.
7. Deb N., *Thermo Chim.Acta*, 320, 1998, 53
8. Bora M.N., Baruah G.C., Talukdar C., *Thermo Chim.Acta*. 218 1993, 425
9. Deb N., Baruah S.D., Das N.N., *Thermo Chim.Acta*, 326, 1999, 43
10. Deb N., Baruah S.D., Sarma N.Sen., Das N.N., *Thermo Chim.Acta*, 338, 1999, 27
11. Deb N., *Thermo Chim.Acta*, 329, 1999, 129
12. Tsuboi.M., *J.Polym.Sci*. 25, 1957, 159
13. Ishikawa, H.; Tsukada, M.; Teizume, I.; Konia, A.; Hirabayashi, K.; Seni, Gakkaishi, 28(4-5), 91(1972)
14. Freeman, E.S. and Carroll, B.; *J.Phys.Chem.*, 62, 394(1958)
